TECHNICAL NOTE

D-549

HEAT-TRANSFER MEASUREMENTS AT A MACH NUMBER OF 4.95 ON TWO 60° SWEPT DELTA WINGS WITH BLUNT LEADING EDGES AND DIHEDRAL ANGLES OF 0° AND 45°

By P. Calvin Stainback

Langley Research Center
Langley Field, Va.

NATIONAL AERONAUTICS AND SPACE ADMINISTRATION

WASHINGTON January 1961

NATIONAL AERONAUTICS AND SPACE ADMINISTRATION

TECHNICAL NOTE D-549

HEAT-TRANSFER MEASUREMENTS AT A MACH NUMBER OF 4.95 ON TWO 60° SWEPT DELTA WINGS WITH BLUNT LEADING EDGES AND DIHEDRAL ANGLES OF 0° AND 45°

By P. Calvin Stainback

SUMMARY

An experimental investigation was conducted to evaluate the heat-transfer characteristics of two 60° swept delta wings with cylindrical leading edges of 0.25-inch radii and dihedral angles of 0° and 45°. The tests were conducted at a Mach number of 4.95 and a stagnation temperature of 400° F. The test-section unit Reynolds number was varied from 1.95×10^6 to 12.24×10^6 per foot.

The results of the investigation indicated that, in a plane normal to the leading edge, the laminar-flow heat-transfer distribution was in good agreement with two-dimensional blunt-body theory. The stagnation-line heat-transfer level could be predicted from two-dimensional blunt-body theory provided the stagnation-line heat-transfer coefficient was assumed to vary as the cosine of the effective sweep.

A comparison of the heating rates to the 0° dihedral wing (planform sweep of 60°) and the 45° dihedral wing (planform sweep of 69.3°) with equal panel sweep and panel area indicated that the stagnation-line heat-transfer coefficient for the 45° dihedral wing could be as much as 40 percent less than the stagnation-line heat-transfer coefficient for the 0° dihedral wing at both equal angles of attack and equal lifts. The laminar-flow heat-transfer rate to both wings outside the vicinity of the stagnation line was essentially equal.

INTRODUCTION

An extensive effort is being made to design winged vehicles suitable for flight at hypersonic speeds. One of the major problems encountered in this endeavor is the high heat-transfer rates to leading edges. Reference 1 described the effects of dihedral on the characteristics of highly swept delta wings and indicated that the leading-edge heat-transfer problem, at angles of attack, could be reduced by the use of positive dihedral. It is the purpose of this report to compare the experimentally determined effects of dihedral on the leading-edge heat-transfer rate to wings with equal panel area and equal panel sweep with the analysis given in reference 1. The report will also present the effects of dihedral on the heating rate to the wing panel rearward of the leading edge and will compare the experimentally determined heating rates for the 0° and 45° dihedral wings at both equal angles of attack and equal lifts. The heat-transfer rate to the ridge line was not assessed in this investigation.

The investigation was conducted at a nominal Mach number of 4.95 and a stagnation temperature of 400° F. The test-section Reynolds number was varied from 1.95×10^{6} to 12.24×10^{6} per foot. The angle of attack was varied from 0° to 20° for the two configurations.

SYMBOLS

C_L	lift coefficient
c_m	specific heat of model material
$\bar{h}$	heat-transfer coefficient, $\dfrac{q}{T_t - T_w}$
h	aerodynamic heat-transfer coefficient, $\dfrac{q}{T_{aw} - T_w}$
M	Mach number
p	pressure
q	aerodynamic heat-transfer rate
q_s	heat storage rate
R	gas constant
r	wing leading-edge radius
s	distance along wing surface (at all angles of attack s is measured from leading-edge stagnation line at $\alpha = 0^{\circ}$)
T	temperature
t	time

V_∞	free-stream velocity
v	local velocity
N_{Re}	unit Reynolds number
α	angle of attack of ridge line
α_{ϵ_e}	angle of attack at which the effective sweeps of leading edge and ridge line are equal
Γ	dihedral angle
δ	flow deflection angle in plane normal to leading edgc
δ_{max}	maximum flow-deflection angle for an attached shock in two-dimensional flow
ϵ_e	angle between leading edges and free stream, effective semiapex angle $\left(\text{complement of } \Lambda_e\right)$
ϵ_n	angle between ridge line and plane of leading edges in vertical plane of symmetry
ϵ_o	angle between ridge line and leading edge in plane of wing, panel semiapex angle
ϵ_p	angle between plane of symmetry and leading edge in plane of leading edges, planform semiapex angle
θ	angle between radius vector to surface and normal component of free-stream velocity
Λ_e	effective sweep of leading edge
Λ_o	complement of ϵ_o
ρ_m	model material density
τ	model material thickness
$\omega = \mu/RT$	
μ	absolute viscosity

Subscripts:

aw	adiabatic wall conditions
c	quantity with constant value
ϵ	outer edge of boundary layer
N	normal to leading edge
s = 0	leading-edge stagnation line at $\alpha = 0^{\circ}$
t	stagnation value
P	parallel to plane of symmetry of model
sl	stagnation line
th	theoretical value
w	wall conditions
α	value at angle of attack
Γ	value at dihedral
∞	free-stream conditions

Superscript:

'	condition behind normal shock

L
9
2
6

MODELS AND TEST PROCEDURE

Models

The models were 60° swept delta wings with blunt leading edges and dihedral angles of 0° and 45°. The leading-edge radii normal to the leading edge were 0.250 inch. The models were formed from identical wing panels and dihedral was introduced into the 45° dihedral model by folding the wing panels about the intersection of the vertical plane of symmetry of the wing and its lower surface. This method of introducing dihedral was called the constant-panel case $\left(\epsilon_o = \text{Constant}\right)$ in reference 1.

The models were fabricated from 0.030-inch-thick type 347 stainless-steel sheet stock to the dimensions given in figure 1. The models were formed from two separate wing panels that were assembled by welding along the plane of symmetry. The wing panels were reinforced with a corrugated filler material to prevent skin deflection due to aerodynamic loading. Care was exercised to insure that none of the filler material was nearer than about 0.25 inch from any thermocouple junction.

The models were instrumented with 0.010-inch-diameter iron-constantan thermocouple wire by spotwelding individual wires to the inside of the model skin. Two thermocouple stations were located on each model. One station was located parallel to the line of symmetry of the model; the other was located normal to the wing leading edge. The location of the individual thermocouples is shown in figure 1. It should be noted that, because of an error in instrumenting the 45° dihedral model, station A, normal to the leading edge, was located approximately 0.40 inch farther from the apex than the same station in the 0° dihedral model. This resulted in the difference between the $(s/r)_N$ values for the ridge line shown in the figures.

Additional physical characteristics of the models are presented in table I. Figure 2 presents a variation of several wing parameters with angle of attack. These parameters include the effective sweep Λ_e, flow deflection angle δ, and the ratio of the cosines of the effective sweep $\cos \Lambda_{e,\Gamma}/\cos \Lambda_{e,\Gamma=0}$, which represents the heat-transfer-coefficient ratio $h_\Gamma/h_{\Gamma=0}$ if the stagnation-line heat-transfer coefficient is assumed to vary as the cosine of the effective sweep.

Test Procedure

Testing of the models was conducted at the Langley Research Center in a 9-inch axially symmetric blowdown jet at a nominal Mach number of 4.95 and stagnation temperature of 400° F. The test-section unit Reynolds number ranged from 1.95×10^6 to 12.24×10^6 per foot.

Testing was performed by the transient heating method. This was accomplished by bringing the jet to the desired operating condition with the model outside the test section. After steady operation was obtained, a vertical door in the test section retracted and the isothermal model, which was mounted on a second door actuated by a horizontal pneumatic cylinder, was inserted into the test section. The time between the instant when the model was just entering the test-section door and the instant when the model was in its proper location in the test section was 0.05 second. The model was removed from the test section after about 4 seconds and brought to isothermal conditions by suitable cooling.

It can be seen from figure 1 that the thermocouples at stations A and B for the flat wing were located on opposite sides of the model. The angle of attack was designated as positive when thermocouples 1 to 5 at station A were on the windward surface. The $(s/r)_N$ values were designated plus and minus on the windward and leeward surfaces, respectively. The 0° dihedral model was tested at negative angles of attack by inverting the model and testing at the same attitudes used for positive angles of attack.

Recording and Reduction of Data

The output of the model thermocouples was recorded on magnetic tape with a Beckman 210-1 digital data recorder. The system sampled and recorded the output of each thermocouple 40 times per second. The data thus recorded represented the temperature time history of the model. These data were reduced to heat-transfer coefficients on an IBM type 650 computer system.

The aerodynamic heat-transfer rate was calculated with the use of the following equation:

$$q = q_s = \rho c_m \tau \frac{\partial T_w}{\partial t} \tag{1}$$

For small initial times, the heat storage rate given by equation (1) represents the aerodynamic heating rate to a high degree of accuracy since lateral conduction and radiation heat-transfer effects are small and normal conduction is sufficiently large to eliminate the effects of normal conduction in the output of the thermocouples located on the inner surface of the model.

In equation (1) the value of ρ_m used was 0.29 lb/cu in., and the value of c_m was 0.12 Btu/(lb)($^{\circ}$F). Because of the small temperature difference experienced during the investigation $\left(\Delta T_{w,max}\right.$ was approximately 40° F; however, a ΔT_w value of 15° F was more $\left.\text{representative}\right)$, the specific heat was assumed to be constant. The model skin thickness was assumed to be equal to the nominal thickness (0.030 inch) of the sheet stock from which the models were fabricated. This value was later confirmed to be correct within ±0.0005 inch by random measurements on the flat surfaces of the models.

The change in temperature with respect to time, required in equation (1), was obtained by fitting a second-degree polynominal to the data, over the time interval of interest, by the method of least squares.

For the present investigation, temperature-time curves were fitted through two groups of data. The first group of data represented the first 20 recorded data points after the initial temperature rise ($0 < t \approx 0.5$ sec); the second group represented the 20 recorded data points immediately after the first group. The equations fitted to the two groups of data were differentiated with respect to time and evaluated at three times within a group. The heat-transfer coefficient for each of the six heat-transfer rates was calculated from the following relation:

$$\bar{h} = \frac{q}{T_t - T_w} \tag{2}$$

It should be noted that in equation (2), the heat-transfer coefficient is defined by using the free-stream total temperature rather than the adiabatic wall temperature.

The heat-transfer coefficients calculated for each group of data were compared with each other for constancy since the coefficient, at a given location, should be essentially constant with respect to time for the small temperature changes experienced. It was found that the agreement between the three heat-transfer coefficients within a group was usually within 10 percent provided $\bar{h} \geqq 0.002$ Btu/(sec)(sq ft)($^{\circ}$F). The maximum deviation in $\bar{h}$ was 20 percent in regions where $\bar{h} \geqq 0.002$ Btu/(sec)(sq ft)($^{\circ}$F). For lower values of $\bar{h}$ ($\bar{h} < 0.002$ Btu/(sec)(sq ft)($^{\circ}$F)), the difference was sometimes substantially higher; however, for these cases the absolute value of $\bar{h}$ was usually small in comparison with the stagnation-line value. The second heat-transfer coefficient for a group, evaluated at the midpoint of the time interval for the group, was chosen to represent the heat-transfer rate for the group. The heat-transfer coefficients used herein were taken from the first group of data except for cases where the percentage difference in the heat-transfer coefficients for the first group was significantly greater than for the second group. The heat-transfer coefficients used are presented in tables II and III.

DISCUSSION OF RESULTS

Heat-Transfer Distribution

The heat-transfer distributions normal to the leading edge for the flat ($\Gamma = 0^{\circ}$) and the 45° dihedral wing are presented in figures 3 and 4. The data are presented in ratio form by dividing the local heat-transfer coefficient $\bar{h}$ by the heat-transfer coefficient at $\left(\frac{s}{r}\right)_N = 0$. The theoretical laminar-flow heat-transfer distribution curves presented in figures 3 and 4 were computed by using the crossflow concept in conjunction with the results of reference 2. The method used to adapt the results of reference 2 to the present configurations is outlined in the appendix.

It should be noted that the heat-transfer coefficient ratio $\bar{h}/\bar{h}_{s=0}$ defined herein is not equivalent to the conventional aerodynamic heat-transfer coefficient ratio. However, for an isothermal model the heat-transfer coefficient used to evaluate the heat-transfer distribution is identical to the heat-transfer rate ratio given in reference 2. The conventional aerodynamic heat-transfer coefficients were not used in this evaluation because of the uncertainty encountered in determining the local adiabatic-wall temperature. This is particularly true on leeward surfaces. It should be further noted that the difference between the conventional aerodynamic heat-transfer coefficient ratio $h/h_{s=0}$ evaluated from Newtonian pressures and isentropic flow considerations and the heat-transfer coefficient ratio $\bar{h}/\bar{h}_{s=0}$ defined herein is less than 7 percent for the conditions encountered during this investigation except for leeward surfaces.

The laminar-flow heat-transfer distribution data shown in figure 3 for the flat wing ($\Gamma = 0^{\circ}$) agreed very well with the theoretical curves for the lower unit Reynolds numbers investigated. (It should be noted that the thermocouple located at s = 0 for station B failed prior to testing (see table II); therefore, the ratios for the distribution shown in figure 3 were obtained by dividing the local heat-transfer coefficient for station B by the heat-transfer coefficient obtained from the thermocouple at s = 0 for station A.) For the higher Reynolds numbers, the agreement between data and theory was good except in regions which appeared to be affected by transition. The displacement of the stagnation line with angle of attack was predicted very well by the flow deflection angle δ. This appeared to be true at $\alpha = 20^{\circ}$ although δ exceeded δ_{max} at $\alpha = 17.57^{\circ}$. (See fig. 2.)

The data obtained from station B, which was parallel to the line of symmetry of the model (fig. 1) also fit the theoretical curve very well. Therefore, it appeared that the wing area surveyed by stations A and B was far enough downstream of the apex to eliminate any influence of the apex on the heat-transfer distribution to this area.

Transition appeared to occur on the flat-wing model as indicated by the rapid increase in the heat-transfer rate with increasing unit Reynolds number for $\left(\frac{s}{r}\right)_N$ values greater than approximately 2. The location of transition appeared to vary with angle of attack; and from the limited amount of data available, it appeared that the transition Reynolds number, based on free-stream conditions and the perpendicular distance from the stagnation line, varied from approximately 7.5×10^5 at $\alpha = 0^\circ$ to 2.5×10^5 at $\alpha = 20^\circ$.

The laminar-flow heat-transfer distribution normal to the leading edge for the 45° dihedral model is presented in figure 4. The data agreed well with the theoretical distribution for the angle-of-attack range investigated. There was some indication at $\alpha = 15^\circ$ and 20° that the heat-transfer rate in the vicinity of the stagnation line was somewhat different than that predicted by theory. Since the flow deflection angle δ exceeded δ_{max} at $\alpha = 11.9^\circ$, it would be expected that the wing panel would have some influence on the flow and, hence, the heat-transfer rate, at the stagnation line. The difference between the data and theory was, however, less than 10 percent; therefore, it cannot be concluded with certainty that the reduction was due to the panel or other effects.

Increases in the apparently laminar-flow heat-transfer rate with distance, in the vicinity of the ridge line, for low unit Reynolds numbers at $\alpha = 15^\circ$ and 20° tend to indicate that the ridge line had become sufficiently unswept to become a detectable leading edge. Since the sweeps of the leading edges and the ridge line become equal at $\alpha_{\epsilon_e} = 20.75^\circ$ (table I), a gradual increase in the heat-transfer rate at the ridge line with increasing angle of attack is expected. Care must be exercised in concluding that the data indicate this trend, since transition can result in similar distributions. For the present investigation, however, the agreement between the data at the two lowest unit Reynolds numbers investigated indicated that the flow was probably laminar and that the increase in the heating rate was due to the ridge line becoming a leading edge.

The displacement of the stagnation line with angle of attack was predicted very well by the flow deflection angle δ. This was true at $\alpha = 15^\circ$ and 20° even though δ exceeded δ_{max} at $\alpha = 11.9^\circ$. (See fig. 2.)

The data obtained from station B, which was parallel to the line of symmetry of the model, agreed with the theoretical curve very well. Thus, it appeared that the heat-transfer distribution on the wing area surveyed by stations A and B was not influenced by the apex of the model.

Transition occurred on the 45° dihedral model as indicated by the rapid increase in the heat-transfer rate with increasing unit Reynolds number $\left(\frac{s}{r}\right)_N$ greater than approximately 2. The location of transition appeared to vary with angle of attack; and it appeared that the transition Reynolds number, based on free-stream conditions and the normal distance from the stagnation line, varied from approximately 5.0×10^5 at $\alpha = 0^\circ$ to 1.8×10^5 at $\alpha = 20^\circ$.

Center-Line and Stagnation-Line Heat-Transfer Level

The heat-transfer level to the leading-edge center line $\left(\frac{s}{r} = 0\right)$ and the stagnation line was evaluated by comparing the measured aerodynamic heat-transfer coefficient with the theoretical values. The aerodynamic heat-transfer coefficient defined as

$$h = \frac{q}{T_{aw} - T_w} \tag{3}$$

was calculated from the measured heat-transfer rates and wall temperatures by estimating the adiabatic-wall temperature from crossflow Newtonian pressure distributions and isentropic flow considerations. The recovery factor was assumed to be equal to the square root of the Prandtl number which was evaluated from the local static temperature. Unpublished pressure data obtained at the Langley Research Center indicated that Newtonian pressure distributions calculated from crossflow considerations agreed with the measured pressure distributions within the flow-deflection-angle range of interest for all test conditions except the 45° dihedral model at angles of attack of 15° and 20°. Therefore, the method used to evaluate the adiabatic-wall temperature appeared to be reasonable in lieu of measured adiabatic-wall temperatures.

The aerodynamic heat-transfer coefficients for the leading-edge center line $\left(\frac{s}{r} = 0\right)$ and the stagnation line are compared with their corresponding theoretical values in figures 5 and 6. The theoretical stagnation-line heat-transfer coefficient for zero sweep was obtained from the results of reference 3 and the stagnation-line heat-transfer coefficient was assumed to vary as the cosine of the effective sweep (ref. 4). The theoretical stagnation-line heat-transfer coefficients, calculated for the angles of attack investigated, are presented in table IV for the flat and the 45° dihedral models.

Since the stagnation-line location varied with angle of attack, direct measurement of the stagnation-line heat-transfer rate was not possible. The stagnation-line heat-transfer coefficients were calculated from the measured center-line $\left(\frac{s}{r} = 0\right)$ heat-transfer coefficients by using the ratio of the stagnation to center-line heat-transfer rate as determined from the flow deflection angle δ. (See appendix.) This procedure appeared reasonable since the distributions discussed in the previous section indicated that the shift in the stagnation-line location could be predicted by δ. It might have been desirable to fair through the data points to obtain the stagnation-line heat-transfer rate; however, it was felt that the instrumentation available was insufficient to warrant this procedure. The theoretical stagnation-line heat-transfer coefficient at $\alpha = 0^{\circ}$ was used to nondimensionalize the stagnation-line heat-transfer data. The results of these calculations are compared in figure 6 with the assumption that the stagnation-line heat-transfer coefficient varies as the cosine of the effective sweep.

The center-line $\left(\frac{s}{r} = 0\right)$ heat-transfer coefficients, presented in figure 5, were nondimensionalized by dividing the measured coefficients by the theoretical stagnation-line heat-transfer coefficient at $\alpha = 0^{\circ}$. The theoretical curve presented in the figure was obtained from the theoretical stagnation-line heat-transfer rate by taking into account the shift in the stagnation line with angle of attack. (See appendix.)

From figures 5 and 6, it is seen that the center-line and stagnation-line heat-transfer coefficients for the flat wing ($\Gamma = 0^{\circ}$) for positive and negative angles of attack bracketed the theoretical curve. The data indicated that the center-line thermocouple was probably located off the center line in a negative $\left(\frac{s}{r}\right)_N$ direction by about 0.080 inch. When this is taken into account, there is reasonable agreement between the data and theory.

The comparison between the measured center-line and stagnation-line heat-transfer coefficients and theory for the 45° dihedral wing was good except for low measured heating rates at $\alpha = 0^{\circ}$. The low heating rates at $\alpha = 0^{\circ}$ could be due to the mutual interference effects of the two leading edges or from apex effects. However, the agreement between the distributions from stations A and B tends to discount this argument unless it is assumed that the interference effects resulted in a general lowering of the heating rate to the entire wing.

In general, the stagnation-line heat-transfer level, the shift in the stagnation line with angle of attack, and the reduction in the stagnation-line heat-transfer coefficient, at angles of attack, as a result of incorporating positive dihedral into a constant-panel wing were in agreement with the results of a theoretical study made of highly swept delta wings with large positive dihedral reported in reference 1.

Comparison of the Heat-Transfer Rates to the Two Models

Equal angles of attack.- In order to compare the heat-transfer characteristics of the flat ($\Gamma = 0^\circ$) and the 45° dihedral wing at equal angles of attack, the local heat-transfer coefficients, defined by equation (2), for the two models were divided by the theoretical stagnation-line heat-transfer coefficients, defined by equation (3), at an angle of attack of 0° for corresponding unit Reynolds numbers. The resulting ratios were plotted against $\left(\frac{s}{r}\right)_N$ and are presented in figure 7.

At a given angle of attack, the heat-transfer rate to the 45° dihedral model in the vicinity of the stagnation line was lower than that for the flat wing. This reduction could be as much as 40 percent at $\alpha = 15^\circ$ and 20°. This reduction was in agreement with the results predicted by the theoretical curve of figure 2. A reduction in the stagnation-line heat-transfer rate for the 45° dihedral model was evident at $\alpha = 0^\circ$, where the heating rates of the two models would be expected to be equal. This result was due to the low center-line heat-transfer rates measured on the 45° dihedral wing at 0° angle of attack, shown in figure 5 and discussed in the previous section. The apparent reduction of the heating rate in the vicinity of the stagnation line for the 45° dihedral model at $\alpha = 0^\circ$ was not representative of the conditions to be expected in this region for the two models; however, the agreement between theory and data at other angles of attack (fig. 5) indicated that the reduction noted in figure 7 for angles of attack greater than 0° was representative of the reduction to be expected from the effects of dihedral.

Except for regions in the vicinity of the stagnation line, the laminar heat-transfer rate to the two models was approximately equal. This result tended to indicate that the heat-transfer rate to the wing panel was probably governed by the deflection angle δ, which for the two models was approximately equal for the angle-of-attack range investigated (fig. 2), and that the effect of the effective sweep on the overall heating rate was limited to a region in the vicinity of the stagnation line.

Equal lifts.- The lift of the flat ($\Gamma = 0^\circ$) and the 45° dihedral models was computed by assuming a Newtonian pressure on the model and by assuming the model thickness to be infinitesimal, that is, leading-edge bluntness was neglected. Under these assumptions, the lift coefficient can be expressed as follows:

$$C_L = 2 \cos \alpha \sin^2\alpha \cos^3\Gamma \tag{4}$$

The lift coefficient C_L was based on the panel area of the models. Thus the comparison at equal lifts for the present investigation will be equivalent to the comparison made in reference 1 for the case where the panel semiapex angle ϵ_O was maintained constant as dihedral was introduced. This method introduced dihedral into the flat wing by folding the wing panels about the plane of symmetry while holding the wing panels fixed. The resulting wing with dihedral has the same lower-surface area and panel sweep as the flat wing but the planform area of the dihedral wing is less and the planform sweep is greater than that of the flat wing. As a result of the decrease in the planform area, the dihedral model will require a greater pressure on the wing to provide a lift equal to that of the flat wing with the same panel area. This greater pressure must be obtained by flying the dihedral wing at higher angles of attack.

If equal lift and equal panel areas are assumed for the flat and 45° dihedral models, equation (4) gives

$$\cos \alpha_\Gamma \sin^2\alpha_\Gamma \cos^3\Gamma = \cos \alpha_{\Gamma=0} \sin^2\alpha_{\Gamma=0} \tag{5}$$

Equation (5) was solved to obtain the following variation of the angle of attack for the flat and 45° dihedral models for equal lift:

$\alpha_{\Gamma=45^\circ}$	$\alpha_{\Gamma=0^\circ}$	C_L
10	5.9	0.021
20	11.5	.078

At equal lifts, the characteristics of the two models are different from those shown in figure 2. In order to illustrate this difference, the characteristics presented in figure 2 for equal angles of attack are presented for equal lifts in figure 8.

The heat-transfer coefficients, defined in equation (2), for the two models were compared at equal lift values of 0.021 and 0.078 in figure 9 by dividing the local heat-transfer coefficient $\bar{h}$ by the theoretical stagnation-line heat-transfer coefficient h defined in equation (3), at zero angle of attack, and by plotting the resulting distribution against $\left(\frac{s}{r}\right)_N$. Since the flat wing was not tested at angles of attack of 5.9° and 11.5°, the heating rates for the flat wing were obtained by cross-plotting the data.

From figure 9, it can be seen that the heat-transfer rate to the 45° dihedral model in the vicinity of the stagnation line was less than that for the flat model. The maximum reduction was approximately 40 percent, which was in agreement with the theoretically predicted value presented in figure 8. The laminar heat-transfer rates to the wing panel, rearward of the leading edge, for the flat and 45° dihedral models were approximately equal for equal values of lift.

Discussion of flow domains.- The results of the present investigation, combined with the results of reference 5, indicated that the flow about a dihedral wing can be tentatively divided into three domains. For a given wing these domains vary with angle of attack and can be described as follows:

(1) At low angles of attack the flow turning angle δ is less than δ_{max} and the stagnation line is located on the leading edge. For this domain, the heat-transfer level to the stagnation line and the heat-transfer distribution about the wing can be predicted by two-dimensional blunt-body theory in conjunction with the crossflow concept.

(2) At higher angles of attack the flow turning angle δ is greater than δ_{max} and the stagnation line is on the leading edge. The heat-transfer level and distribution for this domain can also be predicted by two-dimensional theory.

(3) If the angle of attack is sufficiently large, crossflow will be established on the wing with the stagnation line at the ridge line. The heat-transfer level and distribution can then be predicted by two-dimensional theory by assuming that the stagnation line is located on the ridge line.

Domains (2) and (3) are probably separated by one or more additional domains as the stagnation line shifts from the leading edge to the wing panel and ultimately to the ridge line. At angles of attack below those required to establish crossflow over the wing with the stagnation line on the ridge line, it is possible to have stagnation lines on both the leading edges and the ridge line.

CONCLUSIONS

An experimental investigation was conducted to evaluate the heat-transfer characteristics of two 60° swept delta wings with cylindrical leading edges of 0.25-inch radii and dihedral angles of 0° and 45°. The test was conducted at a Mach number of 4.95 and a stagnation temperature of 400° F. The test-section unit Reynolds number was varied from 1.95×10^6 to 12.24×10^6 per foot.

The results of the investigation indicated that the laminar-flow heat-transfer distribution (ratio of local to stagnation-line heating rate) around the wing normal to the leading edge was in good agreement with two-dimensional blunt-body theory. The stagnation-line heat-transfer level could also be predicted from two-dimensional blunt-body theory provided the stagnation-line heat-transfer coefficient was assumed to vary as the cosine of the effective sweep.

The stagnation-line heat-transfer level, the shift in the stagnation line with angle of attack, and the reduction in the stagnation-line heat-transfer rate, at angles of attack, as a result of incorporating positive dihedral into a constant-panel wing were in agreement with the results of a theoretical study made of highly swept delta wings with large positive dihedral reported in NASA MEMO 3-7-59L.

A comparison of the heating rates to the 0° dihedral wing (planform sweep of 60°) and the 45° dihedral wing (planform sweep of 69.3°) with equal panel sweep and panel area indicated that the stagnation-line heat-transfer coefficient for the 45° dihedral wing could be as much as 40 percent less than the stagnation-line heat-transfer coefficient for the 0° dihedral wing at both equal angles of attack and equal lifts. The laminar-flow heat-transfer rate to both wings outside the vicinity of the stagnation line was essentially equal.

Langley Research Center,
National Aeronautics and Space Administration,
Langley Field, Va., August 31, 1960.

APPENDIX

APPLICATION OF TWO-DIMENSIONAL BLUNT-BODY THEORY TO DELTA WINGS WITH DIHEDRAL

The results of reference 2 can be used to obtain the following expression for the laminar-flow heat-transfer distribution around a two-dimensional blunt body:

$$\frac{q}{q_{sl}} = \frac{f(s)}{\sqrt{\left(\frac{1}{V_\infty}\frac{dv_\epsilon}{ds}\right)_{s=0}}} \tag{A1}$$

where

$$f(s) = \frac{\frac{1}{\sqrt{2}}\frac{p}{p'_{sl}}\frac{\omega_\epsilon}{\omega_{\epsilon,sl}}\frac{v_\epsilon}{V_\infty}}{\left(\int_0^s \frac{p}{p'_{sl}}\frac{\omega_\epsilon}{\omega_{\epsilon,sl}}\frac{v_\epsilon}{V_\infty}\,ds\right)^{1/2}}$$

As a result of defining the aerodynamic heat-transfer coefficient in terms of the total temperature and as a result of the models being approximately isothermal at the time data were reduced, equation (A1) for the heat-transfer ratio is approximately equal to the measured heat-transfer-coefficient ratio.

The relationship for the heat-transfer distribution can be reduced in form if it is assumed that the velocity is linear with distance along the surface, that is,

$$\frac{v_\epsilon}{V_\infty} = \frac{1}{V_\infty}\left(\frac{dv_\epsilon}{d\theta}\right)_{\theta=0}\theta$$

and $\frac{\omega_\epsilon}{\omega_{\epsilon,sl}} = 1$ as noted in reference 2. The substitution of these simplifications into equation (A1) gives

$$\frac{q}{q_{sl}} = \frac{\bar{h}}{\bar{h}_{sl}} = \frac{\frac{1}{\sqrt{2}}\theta \frac{p}{p'_{sl}}}{\left(\int_0^\theta \theta \frac{p}{p'_{sl}} d\theta\right)^{1/2}} \tag{A2}$$

The quantities θ and s are measured from the aerodynamic stagnation line, and any shift in the stagnation line with angle of attack must be taken into account when applying equation (A2) to delta wings.

The pressure distribution required in equation (A2) was taken to be a modified form of the Newtonian pressure distribution which can be expressed as

$$\frac{p}{p'_{sl}} = \cos^2\theta + \frac{p_\infty}{p'_{sl}} \sin^2\theta \tag{A3}$$

Substituting equation (A3) into (A2) and integrating gives

$$\frac{\bar{h}}{\bar{h}_{sl}} = \frac{2\theta\left(\cos^2\theta + \frac{p_\infty}{p'_{sl}} \sin^2\theta\right)}{\left[2\theta^2 + 2\theta \sin 2\theta + \cos 2\theta - 1 + \frac{p_\infty}{p'_{sl}}(2\theta^2 - 2\theta \sin 2\theta - \cos 2\theta + 1) + 8\theta\left(\cos^2\theta + \frac{p_\infty}{p'_{sl}} \sin^2\theta\right)\left(\frac{s}{r} - \theta\right)\right]^{1/2}} \tag{A4}$$

Equation (A4) applies for both the cylindrical leading edge and the plane surfaces of the wing panel $\left(\text{i.e.,}\ \theta = \frac{\pi}{2} - \delta\right)$. When applying the equation to the cylindrical leading edge the last term in the denominator is zero and θ varies; for the wing panel the neglected term is retained and $\theta = \theta_c = \frac{\pi}{2} - \delta$. The flow deflection angle δ will be discussed more fully subsequently.

The ratio of the free-stream static pressure to the stagnation pressure behind the normal shock $\left(p_\infty/p'_{sl}\right)$ in equation (A3) was evaluated by using the normal component of the free-stream Mach number which was computed from the following expression for the effective sweep (see ref. 1):

$$\cos \epsilon_e = \sin \Lambda_e = \cos \epsilon_o \cos \alpha + \sin \epsilon_o \sin \alpha \sin \Gamma \tag{A5}$$

The data were reduced to the form $\bar{h}/\bar{h}_{s=0}$; therefore, a comparison with theory at angles of attack other than $\alpha = 0^{\circ}$ could not be made, as a result of the shift in the stagnation line with angle of attack, unless the theoretical heat-transfer distribution was referenced to $h_{s=0}$. For an isolated swept cylinder, the shift in the stagnation line with angle of attack would be equal to the flow deflection angle δ, given in reference 1 as

$$\cos \delta = \frac{\cos \alpha - \cos \epsilon_o \cos \epsilon_e}{\sin \epsilon_o \sin \epsilon_e} \tag{A6}$$

Using the assumption that the stagnation-line shift on the leading edge of a swept delta wing will, for low angles of attack, be equal to that on a swept cylinder, a factor $\bar{h}_{s=0}/\bar{h}_{sl}$ can be calculated from equations (A4) and (A6) to re-reference the theoretical heat-transfer distribution from the stagnation line to $s/r = 0$.

REFERENCES

1. Cooper, Morton, and Stainback, P. Calvin: Influence of Large Positive Dihedral on Heat Transfer to Leading Edges of Highly Swept Wings at Very High Mach Numbers. NASA MEMO 3-7-59L, 1959.

2. Lees, Lester: Laminar Heat Transfer Over Blunt-Nosed Bodies at Hypersonic Flight Speeds. Jet Propulsion, vol. 26, no. 4, Apr. 1956, pp. 259-269, 274.

3. Reshotko, Eli, and Cohen, Clarence B.: Heat Transfer at the Forward Stagnation Point of Blunt Bodies. NACA TN 3513, 1955.

4. Feller, William V.: Investigation of Equilibrium Temperatures and Average Laminar Heat-Transfer Coefficients for the Front Half of Swept Circular Cylinders at a Mach Number of 6.9. NACA RM L55F08a, 1955.

5. Stainback, P. Calvin: Preliminary Heat-Transfer Measurements on a Hypersonic Glide Configuration Having 79.5° Sweepback and 45° Dihedral at a Mach Number of 4.95. NASA TM X-247, 1960.

TABLE I

GEOMETRY OF MODEL

Model designation	Γ, deg	ϵ_o, deg	Λ_o, deg	ϵ_p, deg	ϵ_n, deg	α_{ϵ_e}, deg	$\Lambda_{e,max}$, deg
Flat model	0	30	60	30	0	90	60
45° dihedral model	45	30	60	20.71	22.21	20.75	69.29

TABLE II.- MEASURED HEAT-TRANSFER COEFFICIENTS OF A 60° SWEPT DELTA WING WITH BLUNT LEADING EDGES AND 0° DIHEDRAL ANGLE

$\left[\Lambda_o = 60^\circ;\ M = 4.95;\ r = 0.25 \text{ in.}\right]$

Station	Thermo-couple	$\left(\frac{s}{r}\right)_N$	$\alpha = 0^\circ$								$\alpha = 5^\circ$							
			p_t = 65 psia; T_t = 437° F		p_t = 109 psia; T_t = 432° F		p_t = 223 psia; T_t = 441° F		p_t = 428 psia; T_t = 460° F		p_t = 63 psia; T_t = 422° F		p_t = 113 psia; T_t = 420° F		p_t = 215 psia; T_t = 431° F		p_t = 425 psia; T_t = 448° F	
			$\bar{h}$ (a)	T_w, °F	$\bar{h}$ (a)	T_w, °F	$\bar{h}$ (a)	T_w, °F	$\bar{h}$ (a)	T_w, °F	$\bar{h}$ (a)	T_w, °F	$\bar{h}$ (a)	T_w, °F	$\bar{h}$ (a)	T_w, °F	$\bar{h}$ (a)	T_w, °F
A	1	6.37	0.0005	81	0.0007	86	0.0042	92	0.0073	89	0.0008	87	0.0022	80	0.0061	77	0.0108	88
	2	5.37	------	--	------	--	------	--	------	---	------	--	------	--	------	--	------	--
	3	3.97	.0007	81	.0010	84	.0015	86	.0058	87	.0010	86	.0014	78	.0036	80	.0128	87
	4	2.97	.0008	80	.0012	84	.0016	85	.0029	88	.0012	84	.0016	78	.0024	78	.0107	86
	5	1.97	.0012	81	.0013	84	.0021	86	.0026	84	.0017	85	.0019	77	.0030	75	.0045	82
	6	1.57	.0019	82	.0022	86	.0031	87	.0043	89	.0020	84	.0032	81	.0044	80	.0065	88
	7	.96	.0041	80	.0055	91	.0073	87	.0109	100	.0049	85	.0066	80	.0092	78	.0131	86
	8	.70	.0063	84	.0079	86	.0113	89	.0155	91	.0071	86	.0094	81	.0131	80	.0186	89
	9	.26	.0084	86	.0107	88	.0153	91	.0201	116	.0087	87	.0116	82	.0158	81	.0224	91
	10	0	.0094	87	.0119	89	.0172	92	.0232	95	.0090	87	.0118	83	.0162	82	.0227	91
	11	-.35	------	--	------	--	------	--	------	---	------	--	------	--	------	--	------	--
	12	-.89	.0049	83	.0058	85	.0085	88	.0117	89	.0038	88	.0045	78	.0063	76	.0090	84
	13	-1.31	.0030	85	.0037	88	.0044	86	.0073	94	.0022	86	.0021	78	.0031	76	.0043	82
	14	-1.73	.0014	83	.0016	84	.0025	88	.0030	85	.0009	84	.0010	77	.0016	77	.0020	81
B	15	1.48	0.0026	84	0.0031	89	0.0044	91	0.0062	93	0.0027	86	0.0042	83	0.0051	76	0.0074	85
	16	1.22	.0026	82	.0037	90	.0052	92	.0074	95	.0033	86	.0042	79	.0067	83	.0097	95
	17	0	------	--	------	--	------	--	------	---	------	--	------	--	------	--	------	--
	18	-1.31	.0033	86	.0039	91	.0050	88	.0082	97	.0023	88	.0023	78	.0035	75	.0050	83
	19	-1.61	.0011	81	.0015	86	.0022	87	.0030	87	.0007	86	.0010	79	.0014	76	.0020	84
	20	-2.57	.0010	81	.0013	87	.0019	87	.0032	88	.0006	86	.0008	79	.0014	77	.0017	83
	21	-3.57	.0006	81	.0007	85	.0011	88	.0063	97	.0003	86	.0004	80	.0010	77	.0013	85
	22	-4.57	.0008	81	.0011	85	.0024	90	.0079	100	.0006	87	.0004	81	.0008	79	.0037	84

[a]Values of $\bar{h}$ are given in Btu/(sec)(sq ft)(°F).

TABLE II.- MEASURED HEAT-TRANSFER COEFFICIENTS OF A 60° SWEPT DELTA WING WITH BLUNT LEADING EDGES AND 0° DIHEDRAL ANGLE - *Continued*

$[\Lambda_o = 60^\circ;\ M = 4.95;\ r = 0.25\ \text{in.}]$

Station	Thermo-couple	$\left(\frac{s}{r}\right)_N$	$\alpha = 10^\circ$								$\alpha = 15^\circ$							
			p_t = 66 psia; T_t = 414° F		p_t = 116 psia; T_t = 418° F		p_t = 215 psia; T_t = 430° F		p_t = 420 psia; T_t = 447° F		p_t = 64 psia; T_t = 382° F		p_t = 114 psia; T_t = 390° F		p_t = 215 psia; T_t = 405° F		p_t = 425 psia; T_t = 427° F	
			$\bar{h}$ (a)	T_w, °F	$\bar{h}$ (a)	T_w, °F	$\bar{h}$ (a)	T_w, °F	$\bar{h}$ (a)	T_w, °F	$\bar{h}$ (a)	T_w, °F	$\bar{h}$ (a)	T_w, °F	$\bar{h}$ (a)	T_w, °F	$\bar{h}$ (a)	T_w, °F
A	1	6.37	0.0013	87	0.0026	80	0.0085	85	0.0142	90	0.0014	79	0.0030	83	0.0126	84	0.0195	108
	2	5.37	------	--	------	--	------	--	------	--	------	--	------	--	------	--	------	---
	3	3.97	.0016	86	.0024	80	.0065	81	.0171	88	.0019	80	.0035	83	.0115	82	.0240	111
	4	2.97	.0015	85	.0023	78	.0034	83	.0167	88	.0022	80	.0031	83	.0068	87	.0253	114
	5	1.97	.0022	83	.0029	80	.0041	83	.0077	91	.0027	80	.0038	83	.0054	84	.0109	92
	6	1.57	.0032	86	.0042	81	.0050	80	.0084	91	.0034	78	.0051	85	.0067	79	.0098	81
	7	.96	.0061	84	.0080	79	.0110	83	.0164	87	.0074	80	.0101	82	.0137	83	.0193	85
	8	.70	.0082	85	.0108	80	.0147	84	.0214	90	.0091	80	.0112	94	.0168	84	.0235	87
	9	.26	.0089	85	.0117	80	.0161	85	.0235	90	.0093	80	.0123	83	.0169	84	.0233	86
	10	0	.0083	85	.0106	91	.0151	84	.0223	90	.0080	80	.0107	82	.0147	83	.0205	85
	11	-.35	------	--	------	--	------	--	------	--	------	--	------	--	------	--	------	---
	12	-.89	.0025	82	.0037	80	.0047	79	.0074	89	.0022	78	.0029	80	.0034	77	.0051	78
	13	-1.31	.0015	84	.0013	76	.0025	81	.0035	84	.0005	77	.0013	79	.0017	78	.0022	80
	14	-1.73	.0004	83	.0010	77	.0008	79	.0013	81	.0002	77	.0003	78	.0005	77	.0007	79
B	15	1.48	0.0040	89	0.0055	83	0.0070	81	0.0102	85	0.0050	83	0.0067	87	0.0088	81	0.0134	85
	16	1.22	.0047	90	.0062	84	.0079	81	.0116	85	.0051	79	.0074	81	.0101	81	.0148	85
	17	0	------	--	------	--	------	--	------	--	------	--	------	--	------	--	------	---
	18	-1.31	.0012	84	.0017	76	.0025	78	.0036	81	.0008	77	.0017	87	.0022	79	.0029	82
	19	-1.61	.0004	84	.0007	76	.0008	79	.0012	82	.0002	77	.0002	78	.0004	78	.0005	80
	20	-2.57	.0005	85	.0004	78	.0009	80	.0011	83	.0002	77	.0004	78	.0007	78	.0003	81
	21	-3.57	.0001	86	.0003	79	.0003	82	.0005	86	.0002	77	.0003	79	.0005	79	.0002	82
	22	-4.57	.0001	86	.0003	81	.0004	84	.0006	88	.0003	77	.0004	79	.0002	81	.0002	84

[a]Values of $\bar{h}$ are given in Btu/(sec)(sq ft)(°F).

TABLE II.- MEASURED HEAT-TRANSFER COEFFICIENTS OF A 60° SWEPT DELTA WING WITH BLUNT LEADING EDGES AND 0° DIHEDRAL ANGLE - Continued

[$\Lambda_o = 60^\circ$; $M = 4.95$; $r = 0.25$ in.]

Station	Thermo-couple	$\left(\frac{s}{r}\right)_N$	$\alpha = -5^\circ$								$\alpha = -10^\circ$							
			p_t = 65 psia; T_t = 399° F		p_t = 111 psia; T_t = 407° F		p_t = 214 psia; T_t = 425° F		p_t = 425 psia; T_t = 448° F		p_t = 66 psia; T_t = 405° F		p_t = 109 psia; T_t = 413° F		p_t = 210 psia; T_t = 420° F		p_t = 425 psia; T_t = 445° F	
			$\bar{h}$ (a)	T_w, °F	$\bar{h}$ (a)	T_w, °F	$\bar{h}$ (a)	T_w, °F	$\bar{h}$ (a)	T_w, °F	$\bar{h}$ (a)	T_w, °F	$\bar{h}$ (a)	T_w, °F	$\bar{h}$ (a)	T_w, °F	$\bar{h}$ (a)	T_w, °F
A	1	-6.37	0.00031	80	0.00075	79	0.00185	80	0.00392	82	0.00048	81	0.00077	80	0.00109	81	0.00187	82
	2	-5.37	-------	--	-------	--	-------	--	-------	---	-------	--	-------	--	-------	--	-------	---
	3	-3.97	.00040	80	.00050	79	.00070	79	.00202	80	.00015	80	.00025	79	.00034	81	.00049	81
	4	-2.97	.00050	80	.00059	79	.00082	79	.00117	80	.00023	80	.00037	79	.00063	80	.00077	81
	5	-1.97	.00058	79	.00085	79	.00108	78	.00165	79	.00043	80	.00048	79	.00077	80	.00148	82
	6	-1.57	.00111	81	.00132	79	.00196	80	.00324	83	.00059	80	.00128	80	.00127	80	.00272	83
	7	-.96	.00306	81	.00378	79	.00518	79	.00921	84	.00219	81	.00307	81	.00664	88	.01206	97
	8	-.70	.00545	82	.00668	81	.00914	81	.01710	90	.00445	86	.00560	83	.01152	85	.02132	91
	9	-.26	.00802	83	.00996	82	.01384	97	.02604	96	.00715	83	.00921	87	.02118	89	.03765	100
	10	0	.00968	85	.01235	84	.01684	86	.03210	101	.00943	85	.01178	90	.02943	94	.05073	109
	11	.35	-------	--	-------	--	-------	--	-------	---	-------	--	-------	--	-------	--	-------	---
	12	.89	.00609	82	.00782	81	.01105	82	.02149	93	.00720	83	.00922	87	.02336	90	.04066	103
	13	1.31	.00360	81	.00472	80	.00652	80	.01408	101	.00497	87	.00611	84	.01350	86	.02750	121
	14	1.73	.00211	80	.00263	79	.00401	83	.00967	93	.00290	84	.00342	82	.00850	83	.01890	90
B	15	-1.48	0.00149	81	0.00191	80	0.00271	81	0.00399	84	0.00097	81	0.00157	80	0.00138	80	0.00176	81
	16	-1.22	.00180	81	.00235	80	.00350	80	.00497	84	.00132	81	.00141	79	.00240	81	.00273	81
	17	0	------	--	------	--	------	--	------	---	------	--	------	--	------	--	------	---
	18	1.31	.00401	81	.00544	86	.00756	89	.01063	87	.00488	83	.00628	85	.00841	84	.01338	88
	19	1.61	.00190	83	.00237	84	.00346	86	.00697	90	.00236	82	.00322	83	.00406	83	.00845	86
	20	2.57	.00136	81	.00207	81	.00265	80	.00954	86	.00218	82	.00275	82	.00368	82	.01560	90
	21	3.57	.00093	81	.00143	79	.00427	80	.01363	89	.00154	82	.00236	82	.00735	91	.01609	90
	22	4.57	.00108	82	.00191	79	.00630	82	.01274	88	.00197	84	.00346	83	.01066	86	.01693	90

[a]Values of $\bar{h}$ are given in Btu/(sec)(sq ft)(°F).

TABLE II.- MEASURED HEAT-TRANSFER COEFFICIENTS OF A 60° SWEPT DELTA WING WITH BLUNT LEADING EDGES AND 0° DIHEDRAL ANGLE - Concluded

[$\Lambda_o = 60^\circ$; $M = 4.95$; $r = 0.25$ in.]

Station	Thermo-couple	$\left(\frac{s}{r}\right)_N$	$\alpha = -15^\circ$						$\alpha = -20^\circ$			
			p_t = 112 psia; T_t = 395° F		p_t = 210 psia; T_t = 408° F		p_t = 419 psia; T_t = 445° F		p_t = 220 psia; T_t = 425° F		p_t = 419 psia; T_t = 444° F	
			$\bar{h}$ (a)	T_w, °F	$\bar{h}$ (a)	T_w, °F	$\bar{h}$ (a)	T_w, °F	$\bar{h}$ (a)	T_w, °F	$\bar{h}$ (a)	T_w, °F
A	1	-6.37	0.00073	75	0.00093	80	0.00106	81	0.00128	81	0.00229	84
	2	-5.37	-------	--	-------	--	-------	---	-------	---	-------	---
	3	-3.97	.00035	75	.00027	79	.00041	80	.00113	82	.00194	83
	4	-2.97	.00029	79	.00026	79	.00039	80	.00104	82	.00157	82
	5	-1.97	.00019	74	.00040	78	.00061	79	.00092	81	.00141	82
	6	-1.57	.00049	75	.00064	79	.00121	81	.00103	81	.00143	82
	7	-.96	.00206	76	.00345	83	.00451	81	.00236	81	.00316	81
	8	-.70	.00450	77	.00620	82	.00933	84	.00545	82	.00768	83
	9	-.26	.00830	79	.01152	85	.01865	89	.01115	86	.01572	88
	10	0	.01176	82	.01627	89	.02188	120	.01532	107	.02088	116
	11	.35	-------	--	-------	--	-------	---	-------	---	-------	---
	12	.89	.01125	81	.01543	89	.02140	117	.01692	112	.02372	122
	13	1.31	.00775	80	.01075	86	.01659	107	.01374	105	.01936	113
	14	1.73	.00445	78	.00640	83	.01189	87	.00894	97	.01623	106
B	15	-1.48	0.00077	76	0.00117	79	0.00171	81	0.00096	81	0.00168	82
	16	-1.22	.00087	75	.00137	79	.00262	82	.00135	81	.00184	81
	17	0	-------	--	-------	--	-------	---	-------	---	-------	---
	18	1.31	.00779	79	.01104	89	.01820	92	.01441	89	.02175	93
	19	1.61	.00383	81	.00525	90	.01341	92	.00826	94	.01516	90
	20	2.57	.00346	79	.00503	85	.02202	93	.00779	94	.02984	97
	21	3.57	.00299	79	.01148	86	.02204	92	.01979	93	.03087	98
	22	4.57	.00483	84	.01475	88	.02222	91	.02047	93	.02994	97

[a]Values of $\bar{h}$ are given in Btu/(sec)(sq ft)(°F).

TABLE III.- MEASURED HEAT-TRANSFER COEFFICIENTS OF A 60° SWEPT DELTA WING WITH BLUNT LEADING EDGES AND 45° DIHEDRAL ANGLE

$\left[\Lambda_o = 60^\circ;\ M = 4.95;\ r = 0.25 \text{ in.}\right]$

Station	Thermo-couple	$\left(\frac{s}{r}\right)_N$	$\alpha = 0^\circ$								$\alpha = 5^\circ$							
			p_t = 65 psia; T_t = 400° F		p_t = 115 psia; T_t = 410° F		p_t = 210 psia; T_t = 422° F		p_t = 445 psia; T_t = 453° F		p_t = 64 psia; T_t = 408° F		p_t = 114 psia; T_t = 415° F		p_t = 215 psia; T_t = 428° F		p_t = 433 psia; T_t = 448° F	
			$\bar{h}$ (a)	T_w, °F	$\bar{h}$ (a)	T_w, °F	$\bar{h}$ (a)	T_w, °F	$\bar{h}$ (a)	T_w, °F	$\bar{h}$ (a)	T_w, °F	$\bar{h}$ (a)	T_w, °F	$\bar{h}$ (a)	T_w, °F	$\bar{h}$ (a)	T_w, °F
A	1	7.81	0.00113	87	0.00195	87	0.00500	88	0.00956	93	0.00101	88	0.00194	88	0.00503	89	0.00920	91
	2	6.33	.00075	86	.00165	86	.00521	87	.00922	92	.00087	87	.00183	87	.00519	88	.00888	90
	3	3.93	.00110	87	.00138	84	.00281	88	.01061	92	.00092	87	.00121	86	.00275	86	.01053	91
	4	2.85	.00130	87	.00129	84	.00207	85	.00732	90	.00093	87	.00136	86	.00178	88	.00795	98
	5	1.97	.00145	88	.00171	84	.00263	88	.00416	93	.00141	88	.00179	85	.00259	88	.00387	87
	6	1.31	.00298	87	.00438	89	.00555	87	.00827	90	.00283	87	.00446	90	.00547	87	.00807	89
	7	.79	.00583	89	.00757	87	.01052	89	.01560	94	.00566	88	.00763	87	.01074	100	.01552	94
	8	.44	.00733	90	.00963	89	.01323	91	.01978	98	.00716	89	.00940	98	.01319	91	.01940	97
	9	0	.00790	91	.01044	89	.01440	92	.02141	99	.00773	90	.01044	89	.01438	92	.02109	98
	10	-.35	.00673	90	.00850	88	.01184	90	.01793	96	.00652	89	.00859	88	.01180	90	.01764	95
	11	-.70	.00498	89	.00628	86	.00870	89	.01346	94	.00471	88	.00626	87	.00879	89	.01304	93
	12	-1.22	.00249	90	.00274	85	.00392	86	.00592	90	.00232	89	.00263	85	.00392	87	.00572	88
	13	-1.57	.00118	87	.00118	84	.00232	88	.00348	92	.00123	88	.00152	86	.00191	86	.00349	90
	14	-2.01	.00072	88	.00091	86	.00121	87	.00194	91	.00061	87	.00087	85	.00113	88	.00196	89
	15	-3.05	.00043	88	.00060	85	.00081	87	.00209	92	.00043	88	.00043	86	.00069	88	.00193	90
	16	-3.97	.00050	88	.00083	86	.00176	89	.00727	93	.00073	89	.00088	86	.00179	90	.00701	91
	17	-5.49	.00039	88	.00063	86	.00164	87	.00587	92	.00053	89	.00040	87	.00154	90	.00581	91
B	18	4.57	0.00093	88	0.00152	89	0.00372	93	0.01153	107	0.00100	90	0.00140	90	0.00342	90	0.01143	105
	19	3.37	.00081	88	.00130	88	.00192	89	.01058	95	.00085	90	.00145	87	.00214	89	.00990	93
	20	2.41	.00111	89	.00144	86	.00220	87	.00834	93	.00113	89	.00149	88	.00214	90	.00619	90
	21	1.48	-------	--	-------	--	-------	---	-------	---	-------	--	-------	--	-------	---	-------	---
	22	1.05	.00335	89	.00455	87	.00625	88	.00894	92	.00375	92	.00459	87	.00621	89	.00877	91
	23	0	.00773	92	.01010	90	.01310	105	.02023	99	.00748	91	.00994	90	.01372	93	.01965	98
	24	-.96	.00324	88	.00445	90	.00555	87	.00859	92	.00349	91	.00448	89	.00549	88	.00831	91
	25	-1.69	-------	--	-------	--	-------	---	-------	--	-------	--	-------	--	-------	---	-------	---
	26	-2.57	.00064	87	.00077	86	.00089	88	.00192	92	.00041	88	.00086	87	.00124	89	.00164	88
	27	-3.93	.00052	88	.00058	87	.00103	89	.00507	98	.00060	89	.00082	87	.00081	90	.00396	91

[a]Values of $\bar{h}$ are given in Btu/(sec)(sq ft)(°F).

TABLE III.- MEASURED HEAT-TRANSFER COEFFICIENTS OF A 60° SWEPT DELTA WING WITH BLUNT LEADING EDGES AND 45° DIHEDRAL ANGLE - Continued

$[\Lambda_o = 60^\circ;\ M = 4.95;\ r = 0.25\ \text{in.}]$

Station	Thermo-couple	$\left(\frac{s}{r}\right)_N$	$\alpha = 10^\circ$								$\alpha = 15^\circ$							
			p_t = 65 psia; T_t = 390° F		p_t = 114 psia; T_t = 394° F		p_t = 220 psia; T_t = 404° F		p_t = 425 psia; T_t = 420° F		p_t = 66 psia; T_t = 380° F		p_t = 113 psia; T_t = 384° F		p_t = 212 psia; T_t = 389° F		p_t = 410 psia; T_t = 412° F	
			$\bar{h}$ (a)	T_w, °F	$\bar{h}$ (a)	T_w, °F	$\bar{h}$ (a)	T_w, °F	$\bar{h}$ (a)	T_w, °F	$\bar{h}$ (a)	T_w, °F	$\bar{h}$ (a)	T_w, °F	$\bar{h}$ (a)	T_w, °F	$\bar{h}$ (a)	T_w, °F
A	1	7.81	0.00215	85	0.00259	84	0.00620	86	0.01228	90	0.00219	83	0.00285	83	0.00416	84	0.01373	90
	2	6.33	.00109	83	.00166	83	.00642	91	.01190	90	.00149	83	.00295	83	.00838	85	.01444	89
	3	3.93	.00124	83	.00216	85	.00716	85	.01430	91	.00149	84	.00266	85	.00686	85	.01653	90
	4	2.85	.00153	84	.00183	84	.00359	87	.01503	92	.00168	84	.00230	85	.00592	89	.02055	92
	5	1.97	.00179	84	.00190	83	.00306	87	.00813	88	.00224	84	.00276	85	.00397	86	.00747	86
	6	1.31	.00373	84	.00482	88	.00702	85	.00933	88	.00427	87	.00540	88	.00723	91	.01034	87
	7	.79	.00593	85	.00743	85	.01105	87	.01515	92	.00551	89	.00759	85	.01037	86	.01488	90
	8	.44	.00693	86	.00873	86	.01268	88	.01749	94	.00622	84	.00800	85	.01087	87	.01563	91
	9	0	.00673	86	.00856	87	.01248	88	.01714	94	.00551	84	.00744	85	.00984	86	.01319	103
	10	-.35	.00521	89	.00676	85	.00992	86	.01312	91	.00346	86	.00508	87	.00676	90	.00941	96
	11	-.70	.00358	84	.00496	88	.00661	85	.00911	88	.00239	82	.00300	82	.00428	83	.00596	85
	12	-1.22	.00125	83	.00207	84	.00286	86	.00426	89	.00083	83	.00120	83	.00136	82	.00232	85
	13	-1.57	.00054	83	.00062	82	.00115	84	.00156	84	.00042	82	.00049	82	.00036	81	.00091	83
	14	-2.01	.00034	83	.00045	83	.00063	84	.00090	84	.00017	82	.00026	82	.00026	82	.00032	82
	15	-3.05	.00029	84	.00037	84	.00018	85	.00063	85	.00011	83	.00007	83	.00009	82	.00036	83
	16	-3.97	.00024	86	.00048	87	.00100	90	.00217	91	.00015	86	.00021	86	.00065	87	.00108	90
	17	-5.49	.00019	93	.00034	93	.00066	96	.00185	99	.00016	95	.00035	95	.00040	95	.00086	97
B	18	4.57	0.00158	85	0.00299	85	0.00824	96	0.01418	92	0.00190	84	0.00444	85	0.01073	88	0.01582	92
	19	3.37	.00099	88	.00160	90	.00434	92	.01334	111	.00139	90	.00263	92	.00752	98	.01496	97
	20	2.41	.00139	84	.00192	85	.00324	88	.00885	89	.00165	85	.00239	83	.00510	85	.01565	91
	21	1.48	-------	--	-------	--	-------	--	-------	---	-------	--	-------	--	-------	--	-------	---
	22	1.05	.00407	88	.00499	85	.00733	87	.00961	89	.00421	87	.00534	85	.00757	86	.01100	89
	23	0	.00665	87	.00850	87	.01169	89	.01554	94	.00500	84	.00679	85	.00986	87	.01376	91
	24	-.96	.00213	83	.00321	86	.00394	84	.00526	86	.00162	83	.00181	82	.00248	82	.00343	84
	25	-1.69	.00081	84	.00105	84	.00133	85	.00142	85	.00020	82	.00039	82	.00045	82	.00112	84
	26	-2.57	.00035	84	.00050	84	.00081	85	.00080	86	.00027	83	.00021	82	.00036	82	.00039	84
	27	-3.39	.00033	84	.00041	84	.00051	86	.00081	86	.00010	83	.00018	83	.00011	83	.00015	84

[a]Values of $\bar{h}$ are given in Btu/(sec)(sq ft)(°F).

TABLE III.- MEASURED HEAT-TRANSFER COEFFICIENTS OF A 60° SWEPT DELTA WING WITH BLUNT LEADING EDGES AND 45° DIHEDRAL ANGLE - Concluded

[$\Lambda_o = 60°$; $M = 4.95$; $r = 0.25$ in.]

Station	Thermo-couple	$\left(\frac{s}{r}\right)_N$	$\alpha = 20°$							
			p_t = 65 psia; T_t = 407° F		p_t = 114 psia; T_t = 410° F		p_t = 210 psia; T_t = 415° F		p_t = 420 psia; T_t = 440° F	
			$\bar{h}$ (a)	T_w, °F	$\bar{h}$ (a)	T_w, °F	$\bar{h}$ (a)	T_w, °F	$\bar{h}$ (a)	T_w, °F
A	1	7.81	0.00371	87	0.00401	85	0.00605	88	0.02375	99
	2	6.33	.00218	83	.00310	84	.01172	90	.02084	118
	3	3.93	.00163	84	.00279	87	.00721	88	.02155	96
	4	2.85	.00185	85	.00258	87	.00544	93	.02527	99
	5	1.97	.00236	84	.00332	88	.00460	91	.01149	100
	6	1.31	.00450	85	.00602	86	.00831	88	.01174	91
	7	.79	.00578	86	.00747	87	.01028	89	.01484	93
	8	.44	.00551	86	.00745	87	.01005	89	.01450	93
	9	0	.00462	85	.00606	86	.00810	88	.01170	92
	10	-.35	.00279	84	.00360	84	.00506	91	.00699	88
	11	-.70	.00186	85	.00233	85	.00274	85	.00446	90
	12	-1.22	.00064	84	.00074	84	.00094	86	.00136	86
	13	-1.57	.00012	83	.00041	83	.00044	85	.00090	85
	14	-2.01	.00010	84	.00028	84	.00032	85	.00051	86
	15	-3.05	.00024	84	.00022	85	.00029	86	.00067	86
	16	-3.97	.00035	89	.00039	90	.00057	92	.00203	95
	17	-5.49	.00029	96	.00042	98	.00083	100	.00162	101
B	18	4.57	0.00214	85	0.00556	87	0.01376	105	0.02083	117
	19	3.37	.00161	92	.00292	92	.01022	97	.01930	103
	20	2.41	.00192	85	.00294	86	.00583	88	.02298	98
	21	1.48	-------	--	-------	--	-------	---	-------	---
	22	1.05	.00467	86	.00621	87	.00864	90	.01242	93
	23	0	.00433	86	.00556	86	.00747	89	.00005	89
	24	-.96	.00104	84	.00102	83	.00130	85	.00161	85
	25	-1.69	.00024	84	.00012	84	.00025	86	.00047	86
	26	-2.57	.00028	84	.00039	84	.00031	86	.00020	86
	27	-3.39	.00056	84	.00049	85	.00018	86	.00020	86

[a]Values of $\bar{h}$ are given in Btu/(sec)(sq ft)(°F).

TABLE IV

STAGNATION-LINE HEAT-TRANSFER COEFFICIENT FOR A 60° SWEPT

WING WITH DIHEDRAL ANGLES OF 0° AND 45°

[$M = 4.95$; $T_t = 400°$ F; $r = 0.25$ in.]

Angle of attack, α, deg	h_{sl}, Btu/(sec)(sq ft)(°F), for -			
	$N_{Re} = 1.95 \times 10^6$	$N_{Re} = 3.39 \times 10^6$	$N_{Re} = 6.34 \times 10^6$	$N_{Re} = 12.24 \times 10^6$
$\Gamma = 0°$				
0	0.01172	0.01558	0.02130	0.02960
5	.01185	.01585	.02154	.02994
10	.01223	.01626	.02224	.03091
15	.01284	.01707	.02334	.03244
20	.01362	.01810	.02475	.03440
$\Gamma = 45°$				
0	0.01172	0.01558	0.02130	0.02960
5	.01052	.01399	.01913	.02658
10	.00949	.01262	.01726	.02398
15	.00873	.01160	.01587	.02205
20	.00838	.01107	.01514	.02104

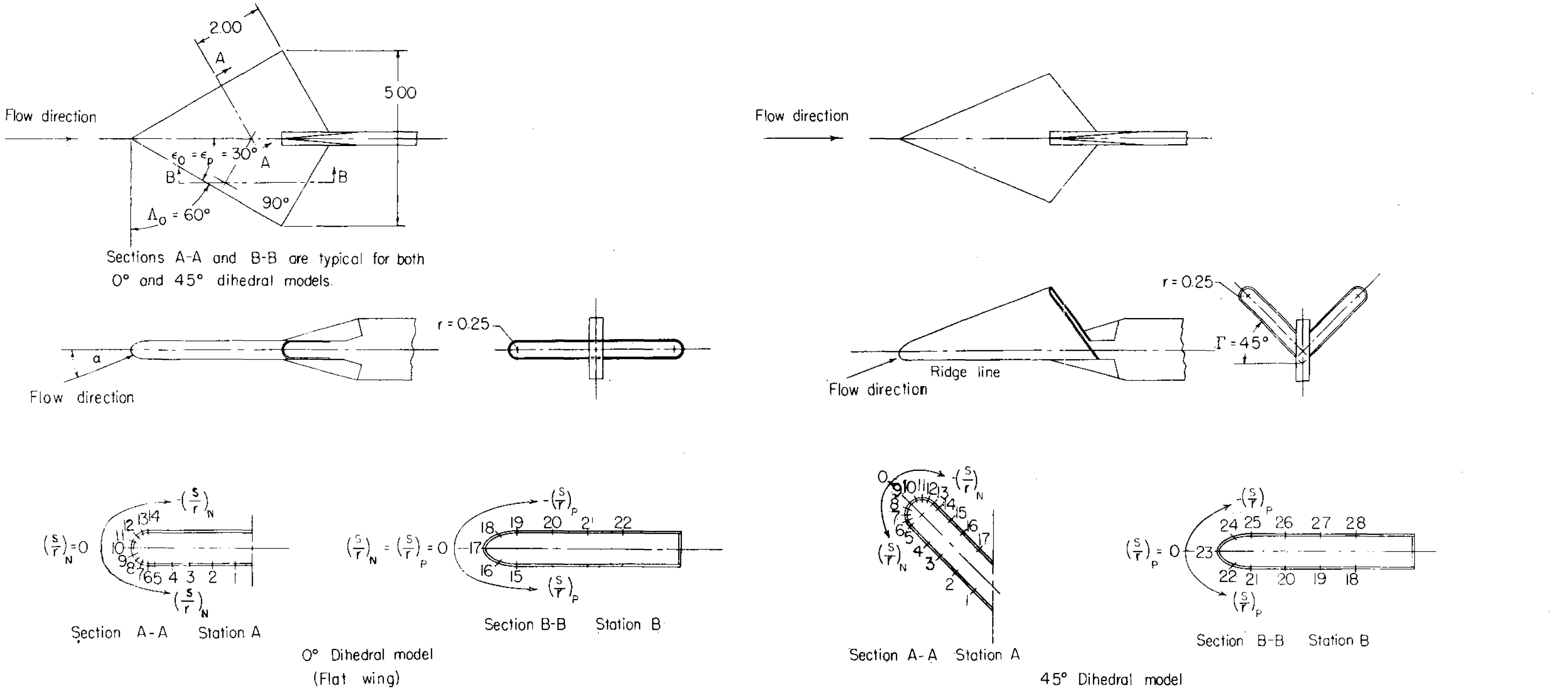

Figure 1.- Geometry and instrumentation of models. The 0° and 45° dihedral models were fabricated from identical wing panels.

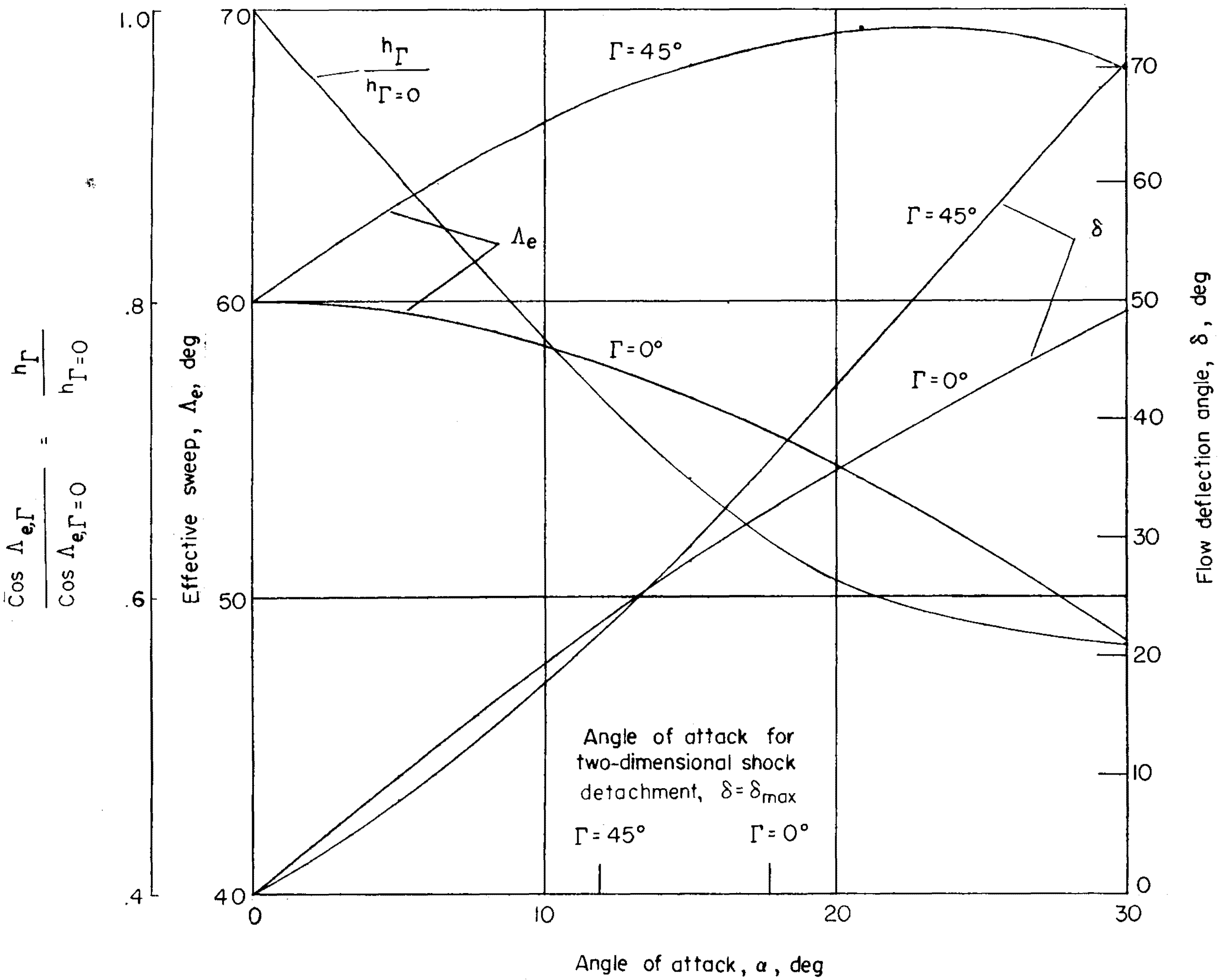

Figure 2.- Variation of wing effective geometry with angle of attack.

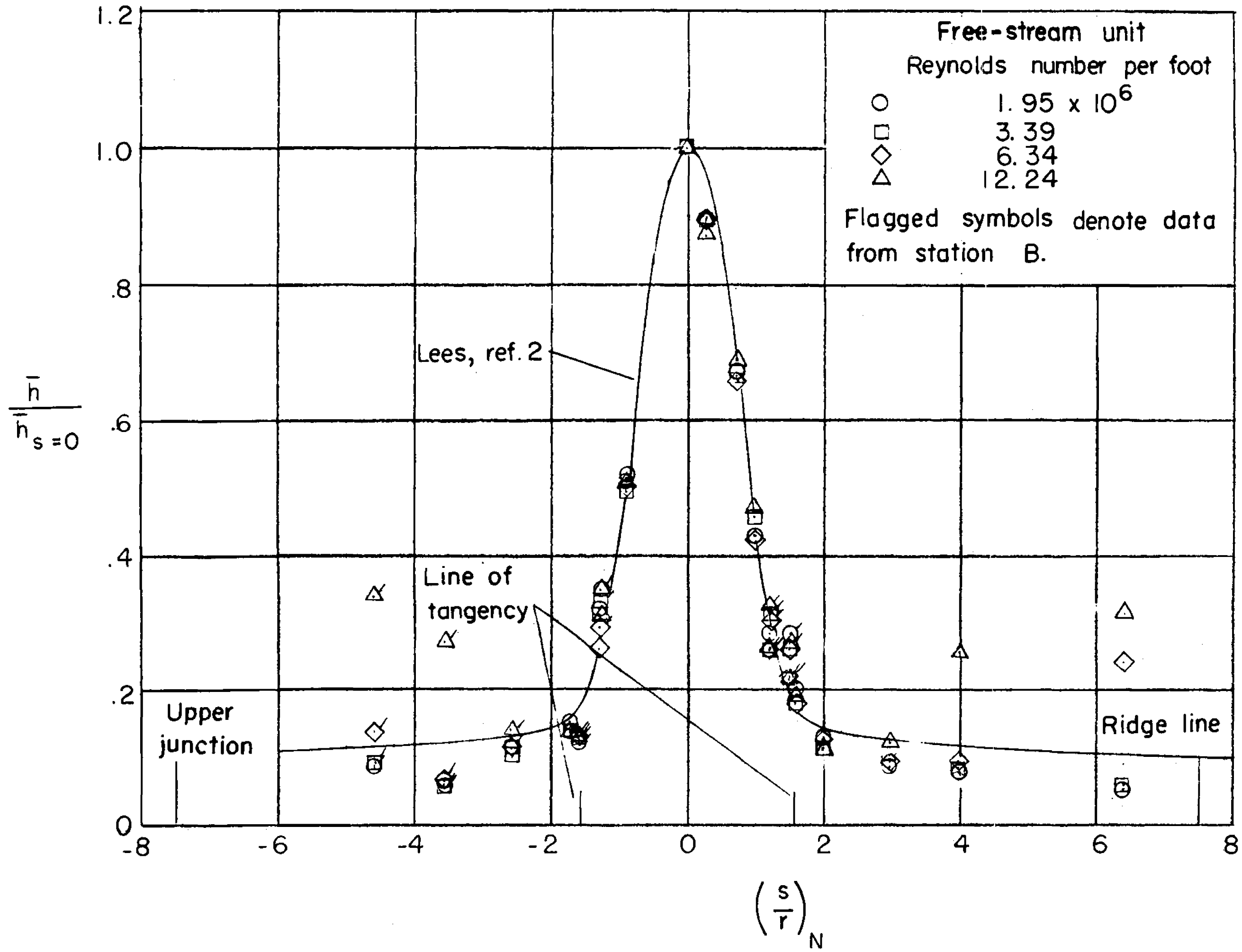

(a) $\alpha = 0^{\circ}$.

Figure 3.- Heat-transfer distribution normal to leading edge for 0° dihedral (flat) wing.

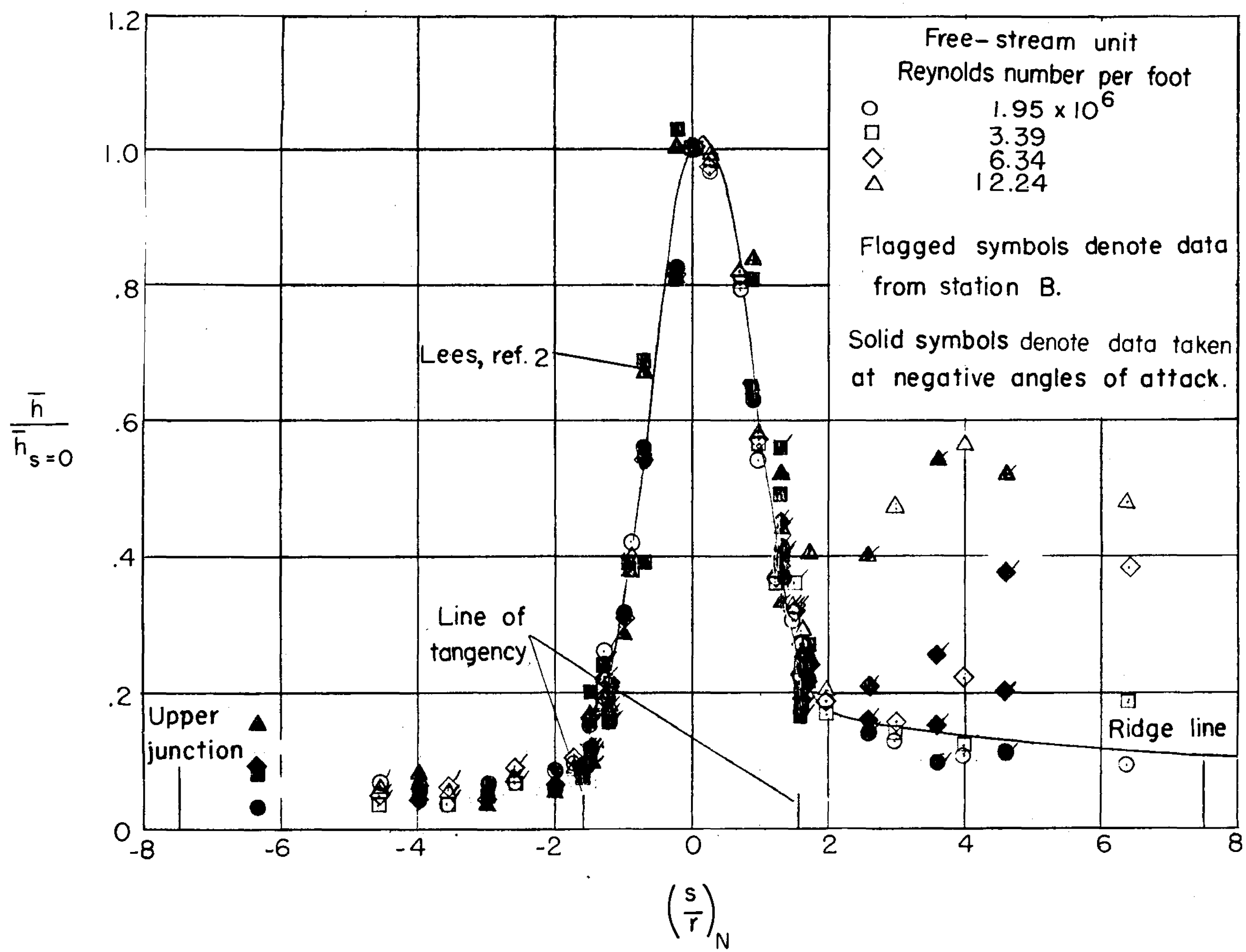

(b) $\alpha = 5^{\circ}$.

Figure 3.- Continued.

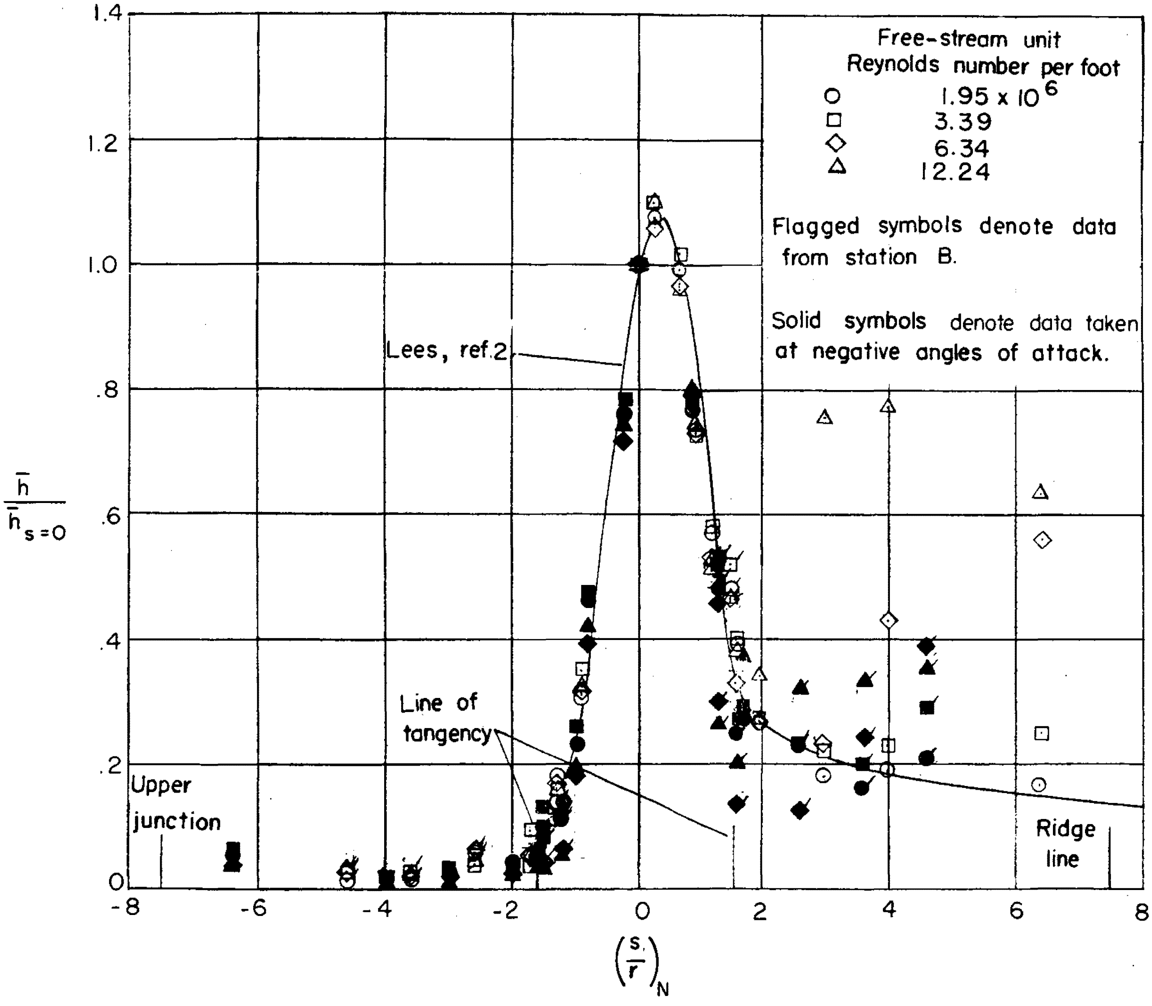

(c) $\alpha = 10^{\circ}$.

Figure 3.- Continued.

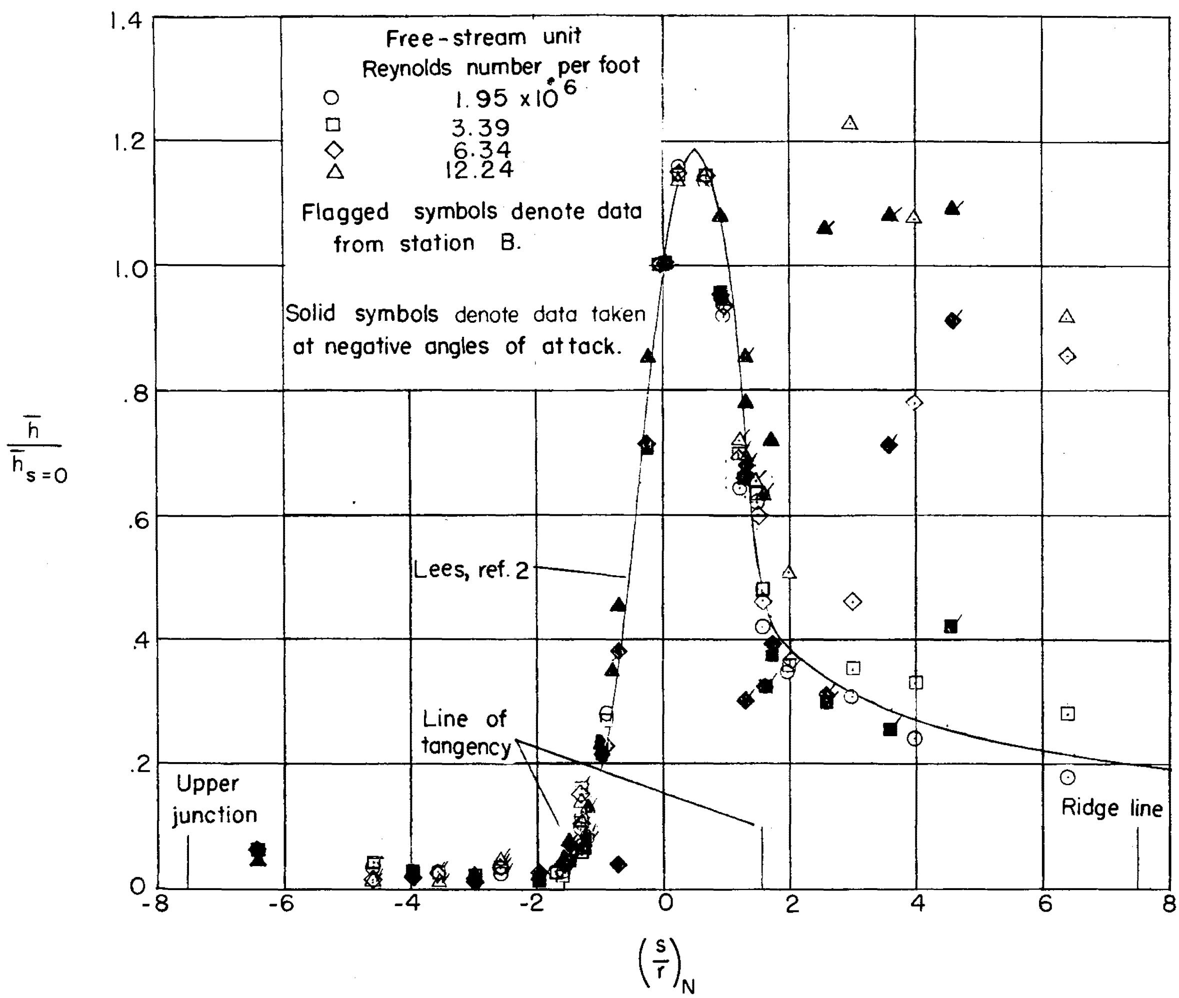

(d) $\alpha = 15^{\circ}$.

Figure 3.- Continued.

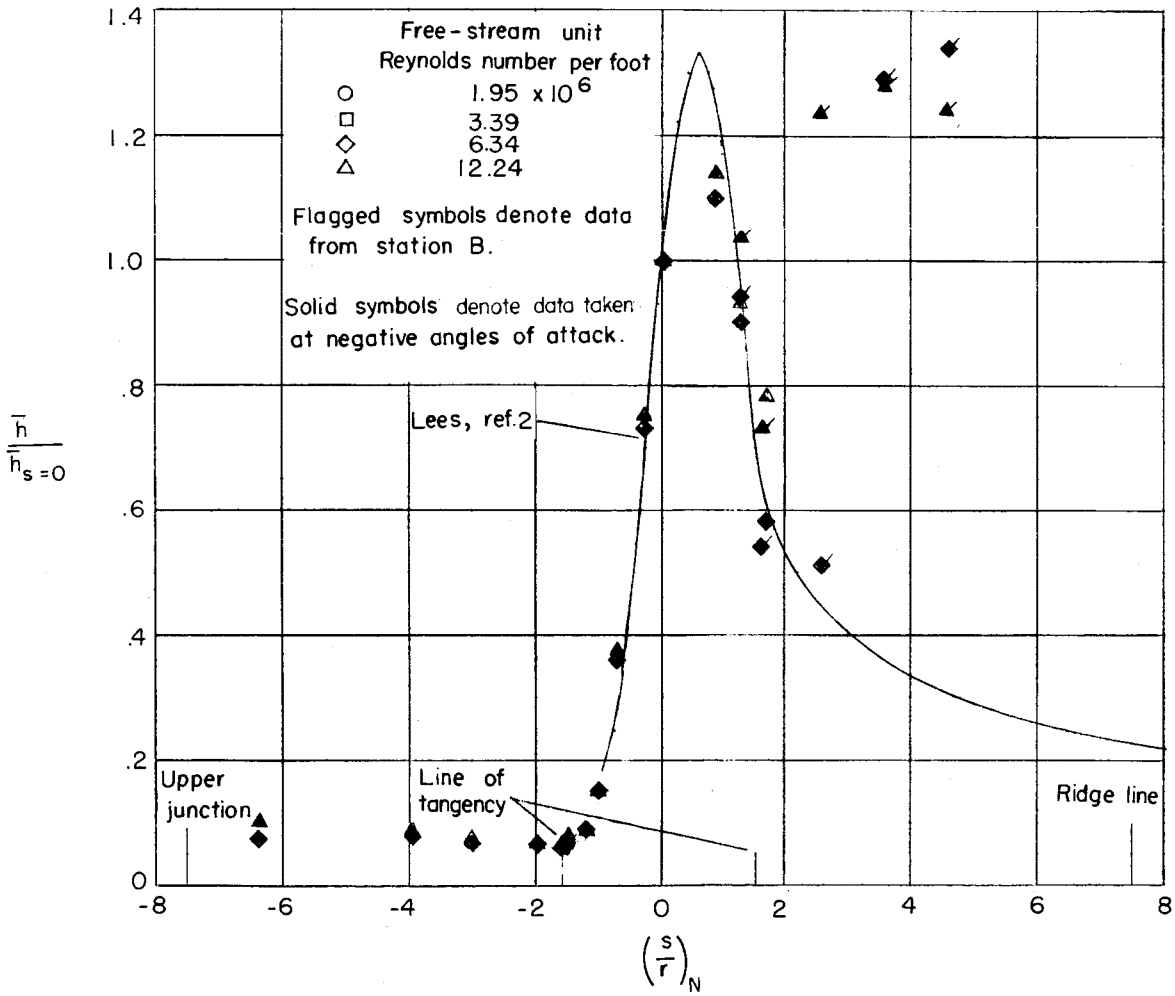

(e) $\alpha = 20^{\circ}$.

Figure 3.- Concluded.

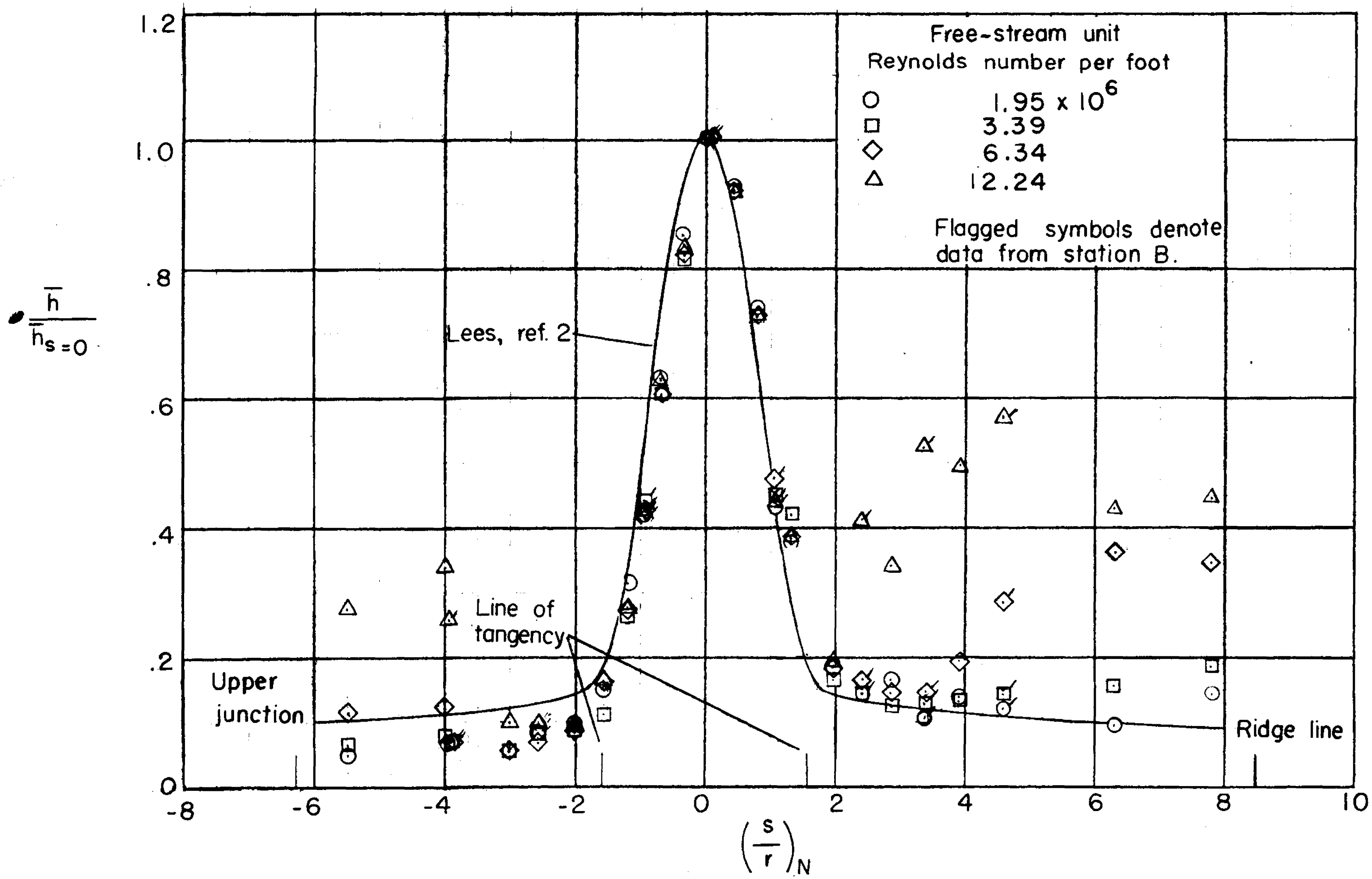

(a) $\alpha = 0^{\circ}$.

Figure 4.- Heat-transfer distribution normal to leading edge for 45° dihedral wing.

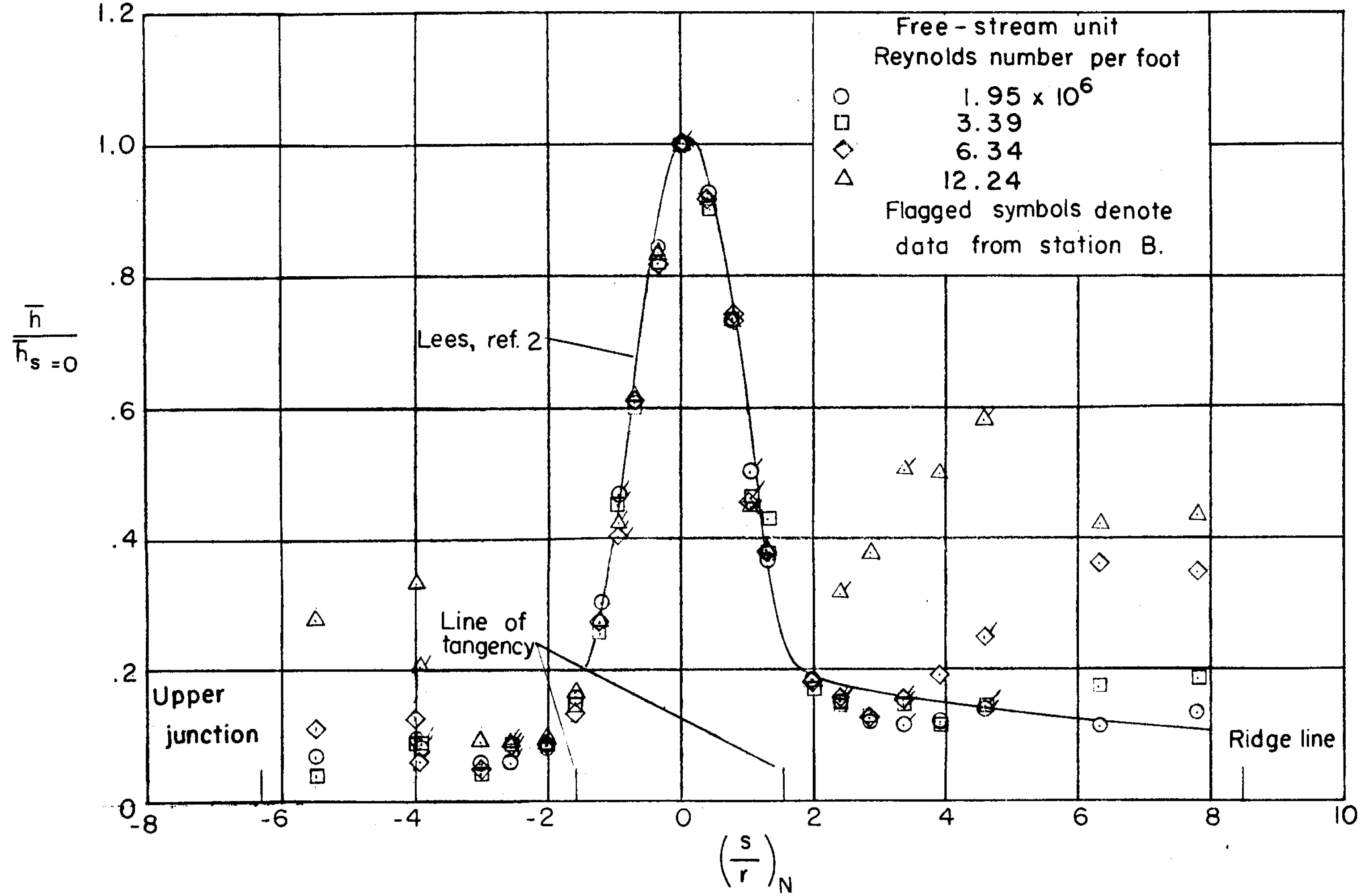

(b) $\alpha = 5^{\circ}$.

Figure 4.- Continued.

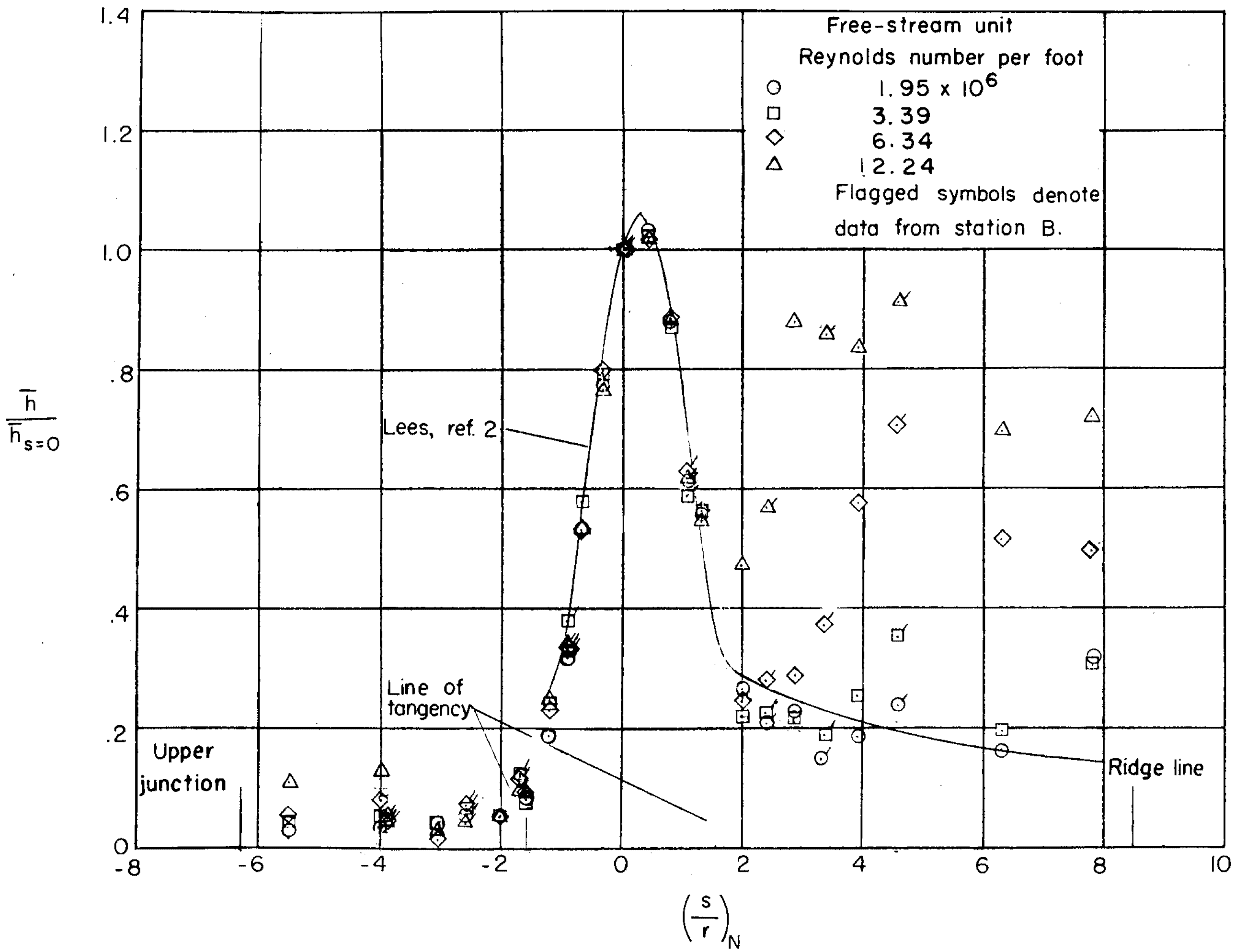

(c) $\alpha = 10^{\circ}$.

Figure 4.- Continued.

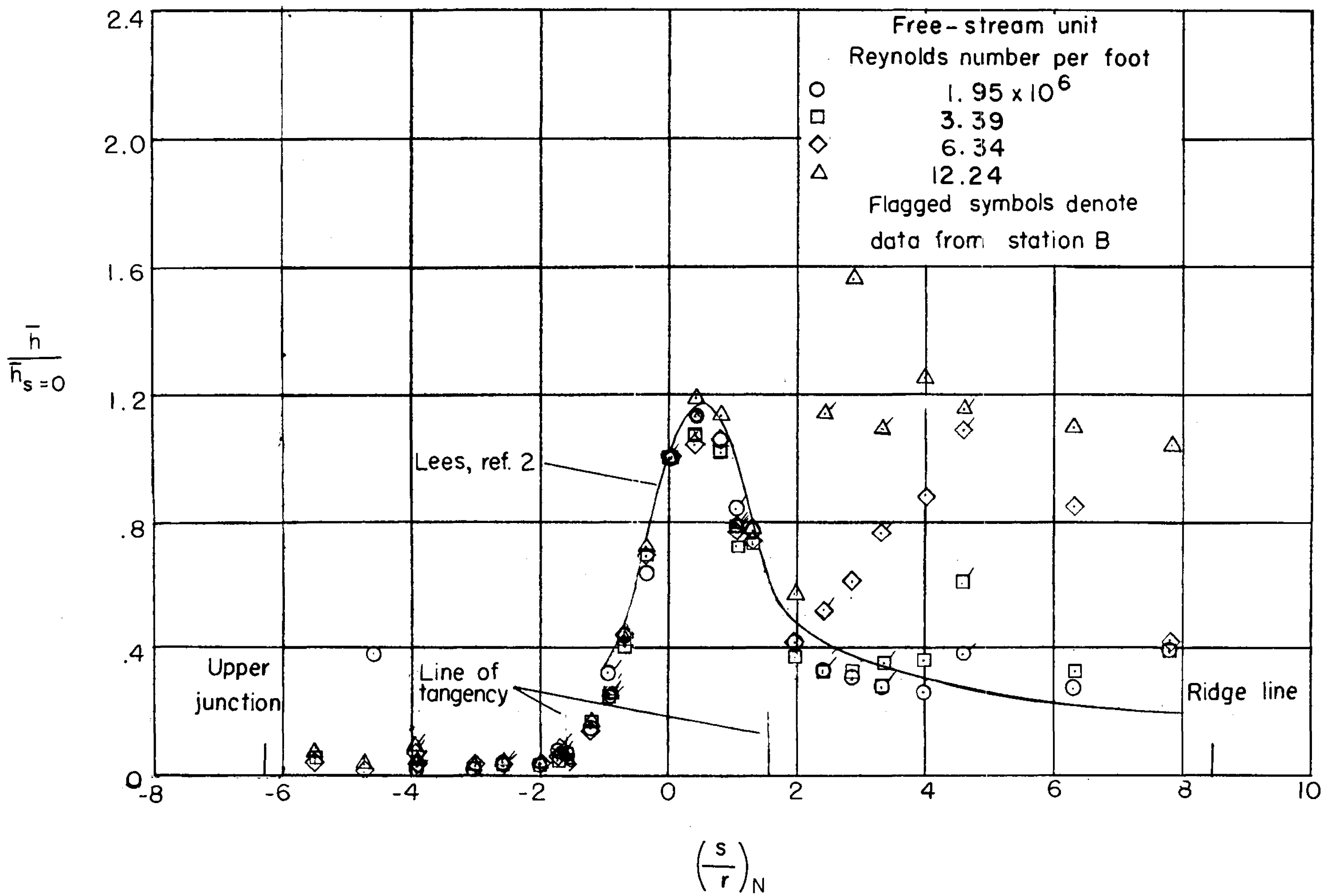

(d) $\alpha = 15^{\circ}$.

Figure 4.- Continued.

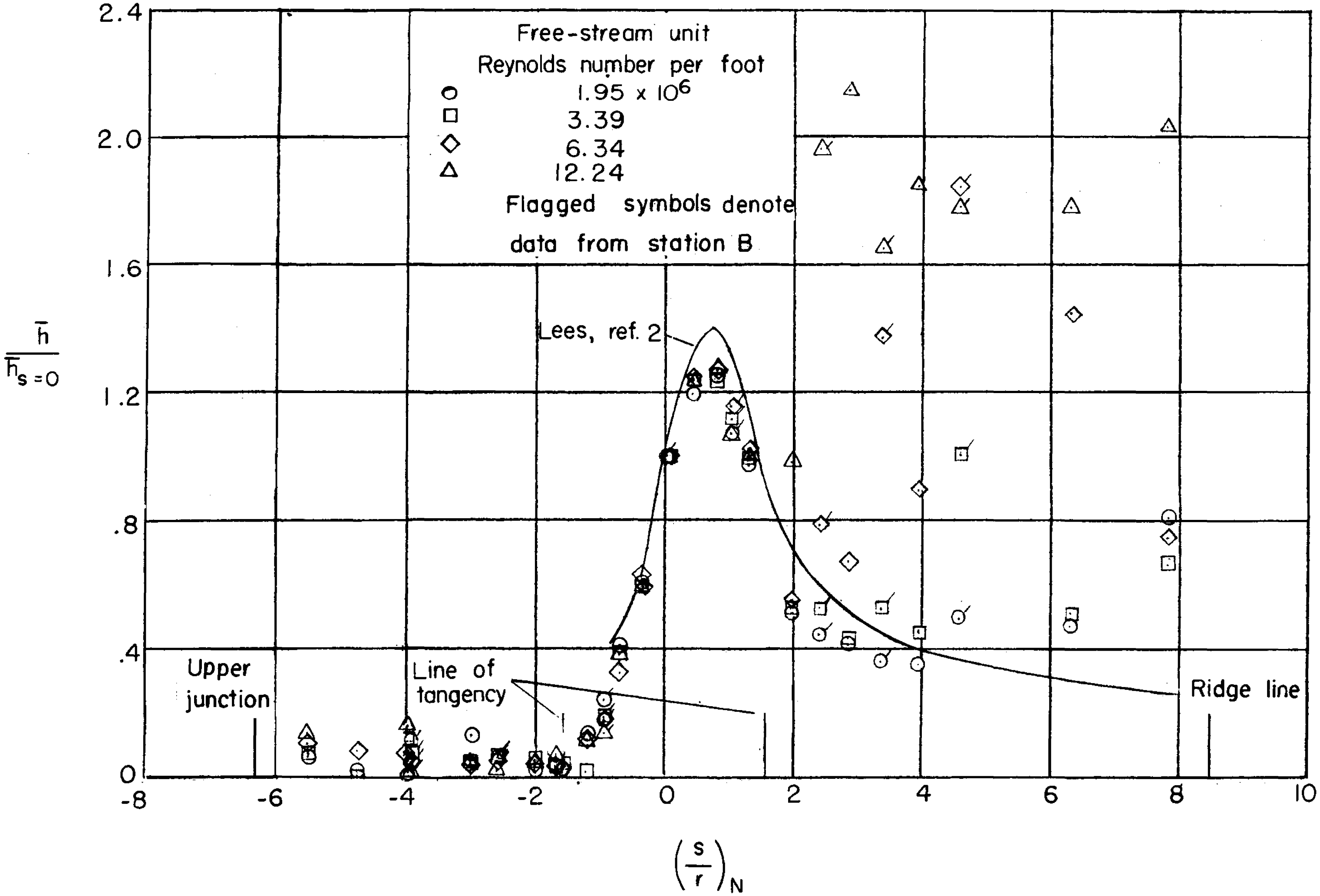

(e) $\alpha = 20^{\circ}$.

Figure 4.- Concluded.

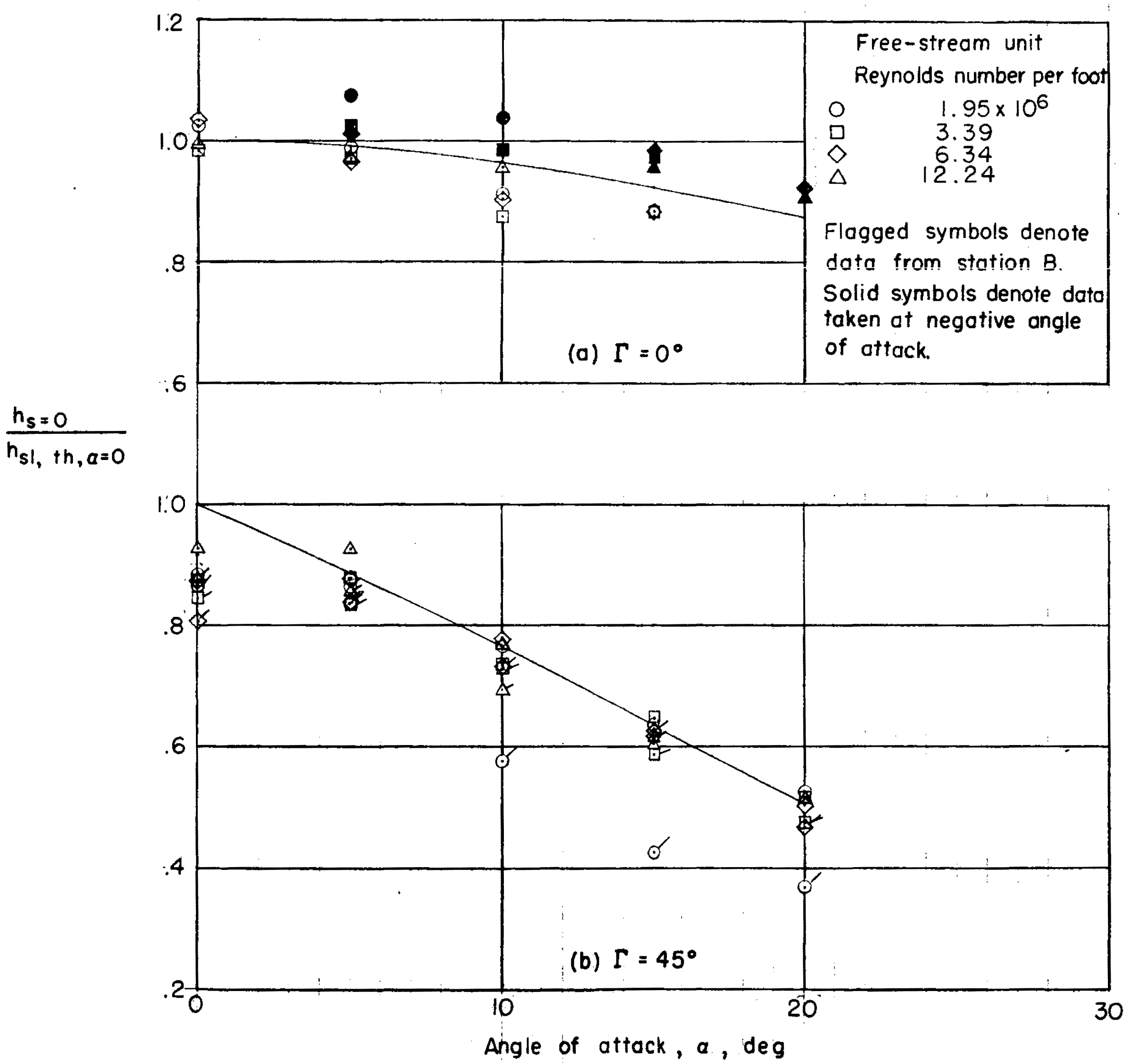

Figure 5.- Heat-transfer rate to the model leading-edge center line ($s/r = 0$).

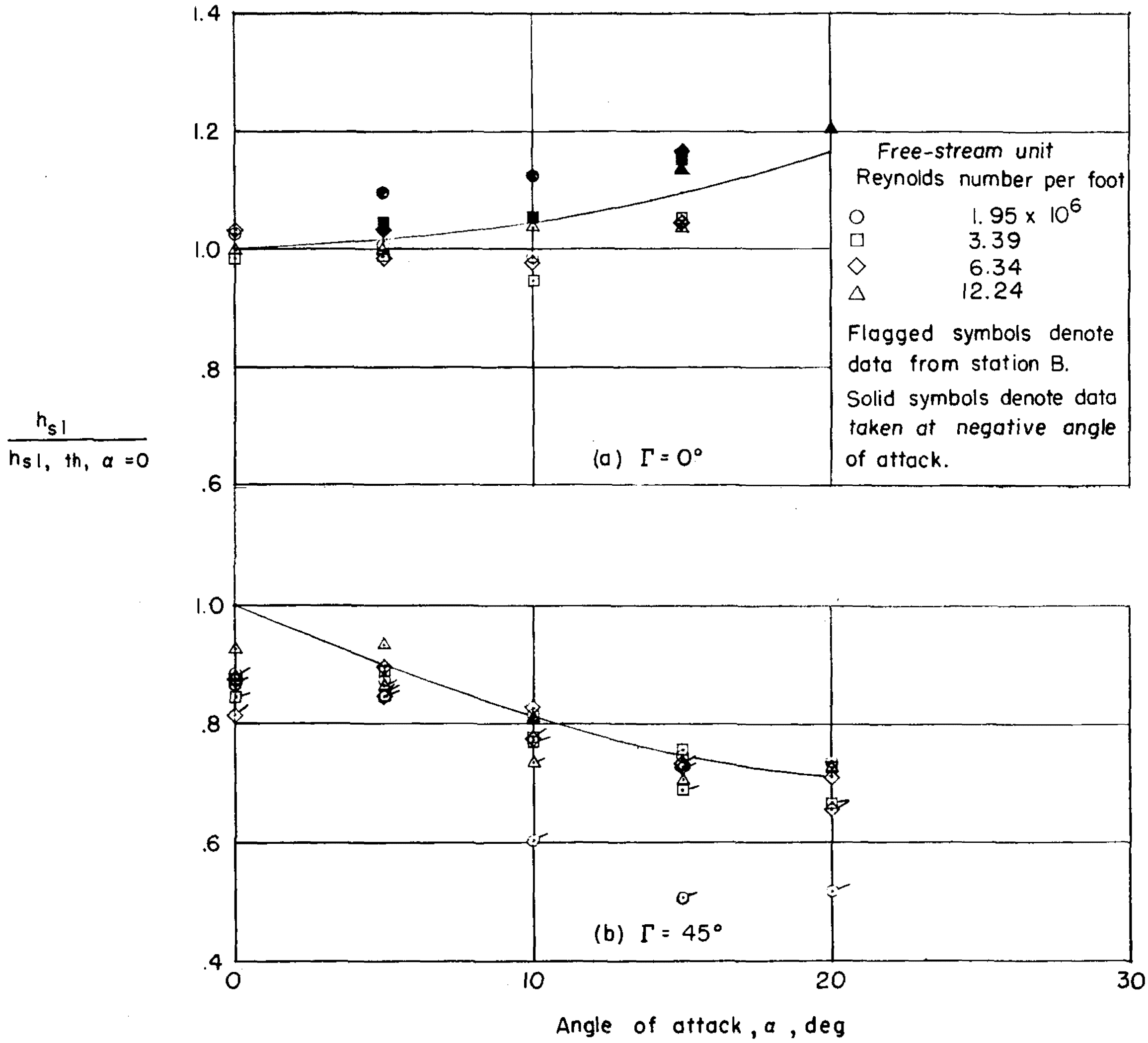

Figure 6.- Stagnation-line heat-transfer rate to 60° swept delta wing.

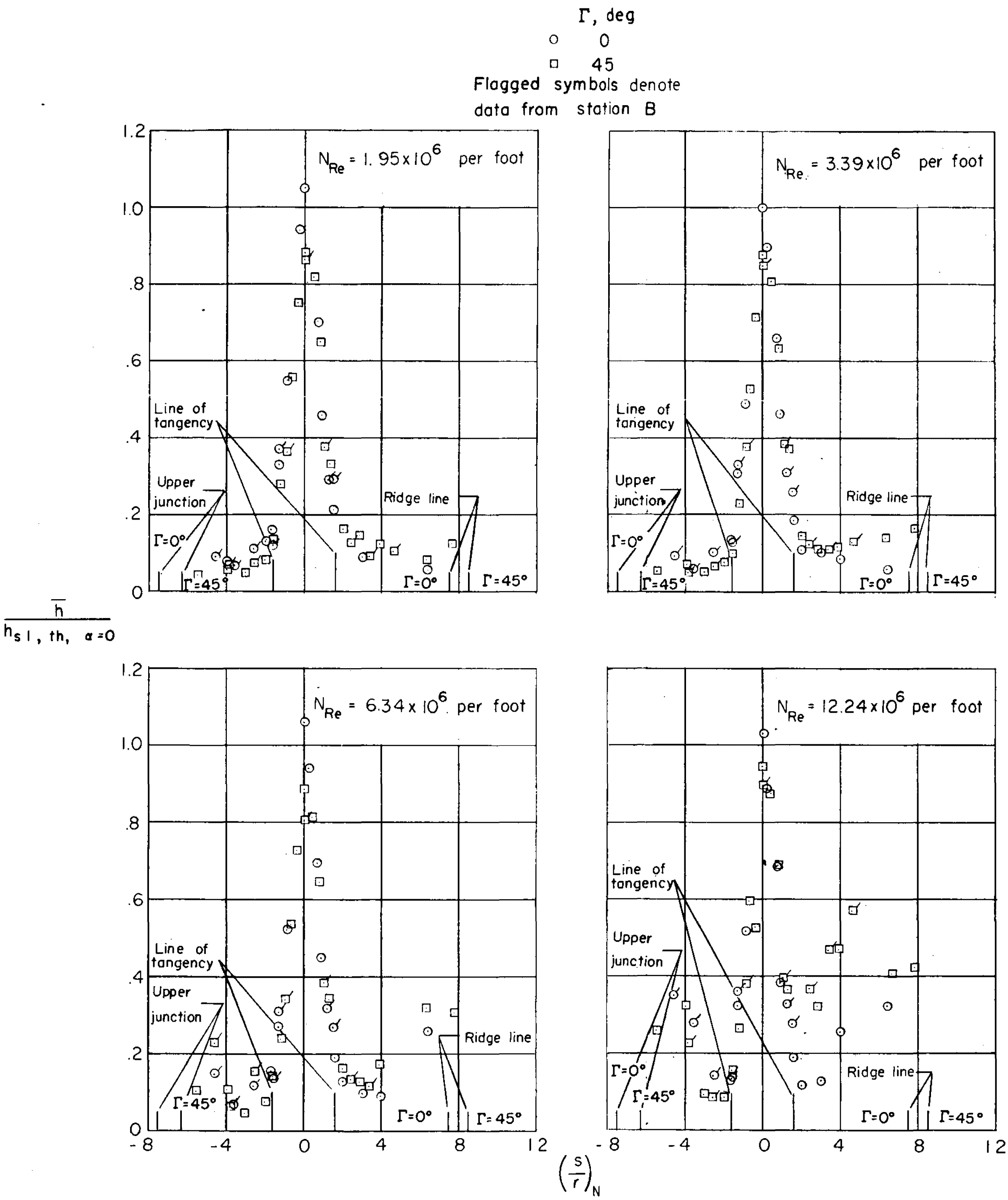

(a) $\alpha = 0^\circ$.

Figure 7.- A comparison of the heating rate to the 0° and 45° dihedral wings at equal angles of attack and equal unit Reynolds numbers.

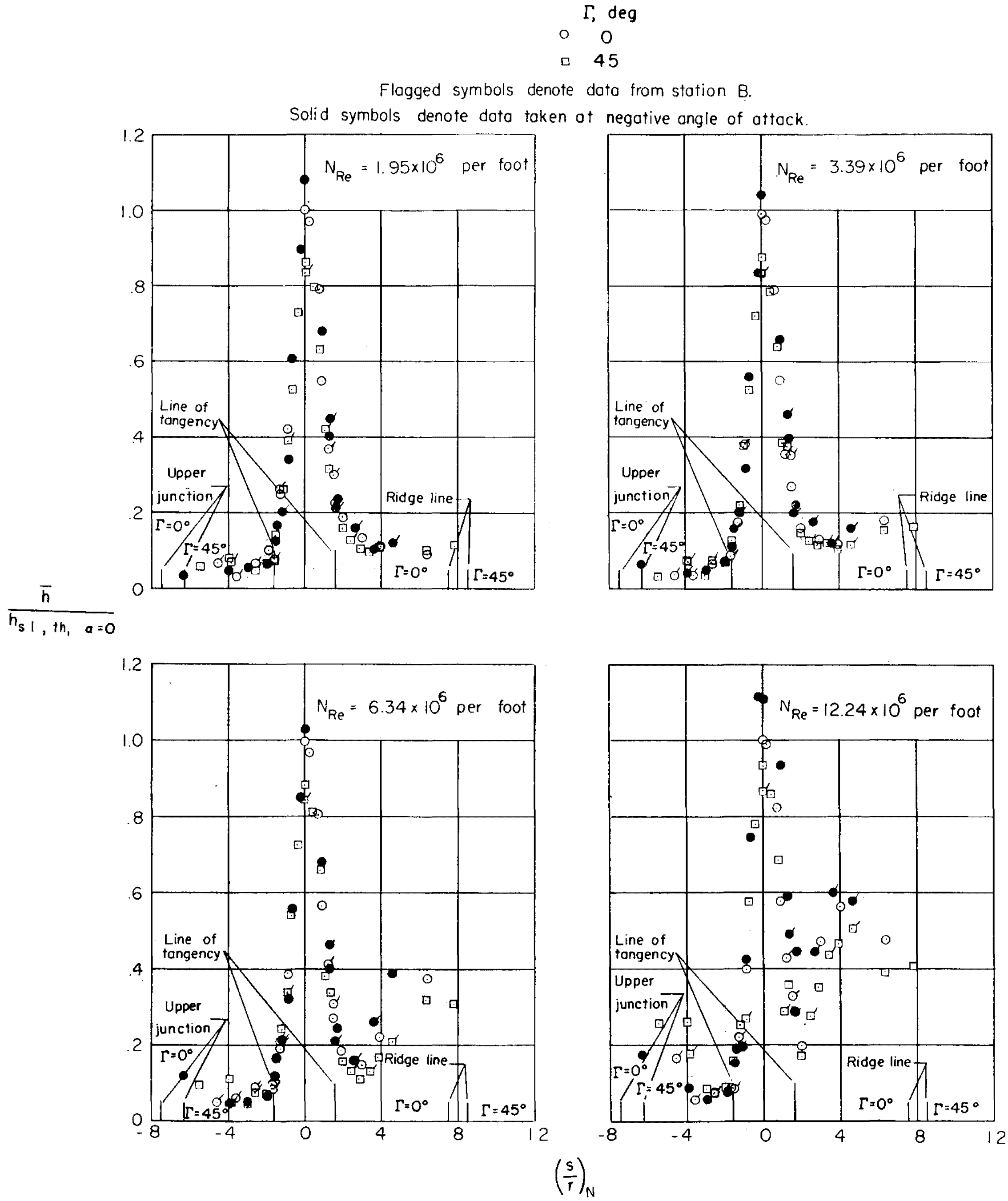

(b) $\alpha = 5^{\circ}$.

Figure 7.- Continued.

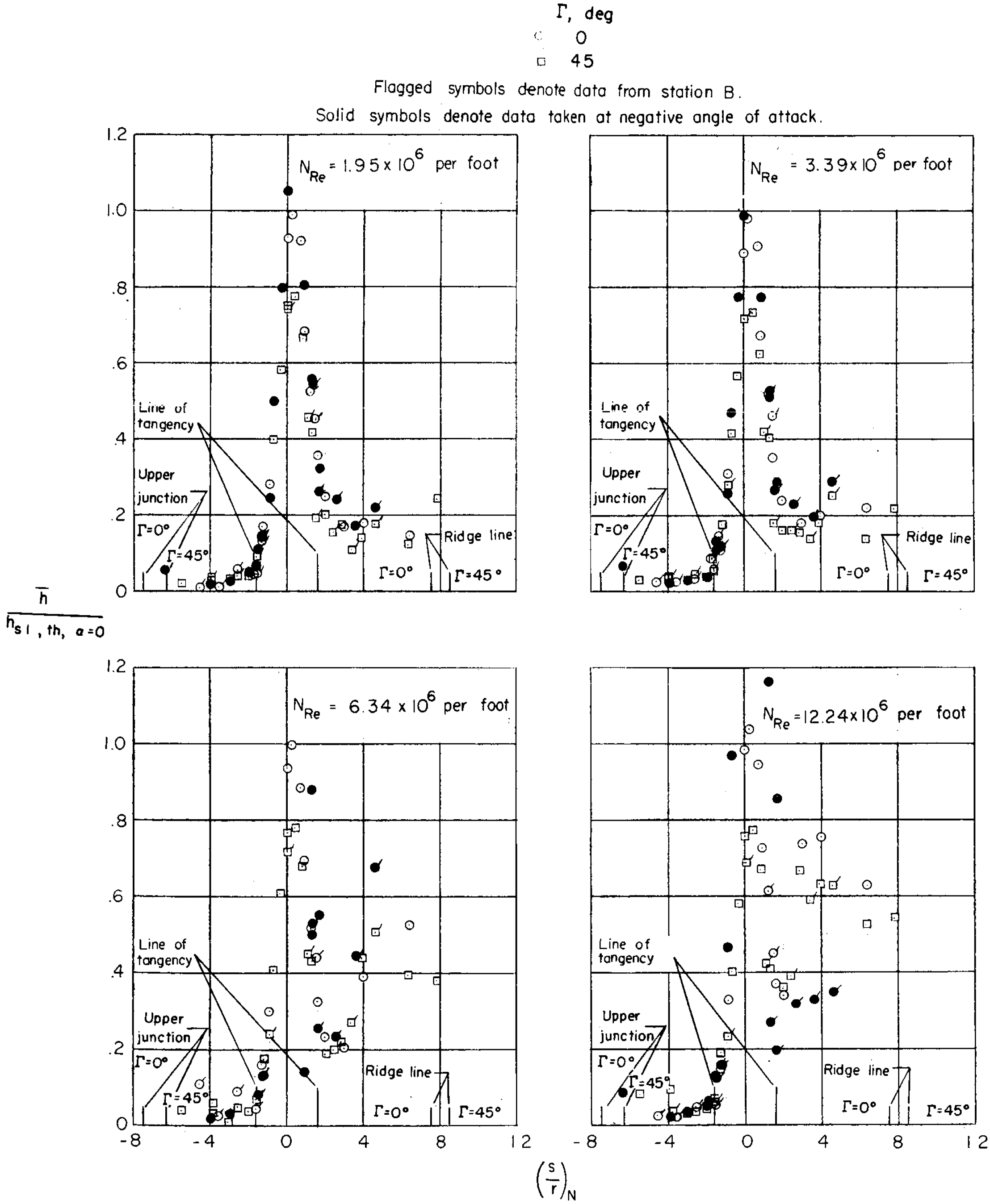

(c) $\alpha = 10^{\circ}$.

Figure 7.- Continued.

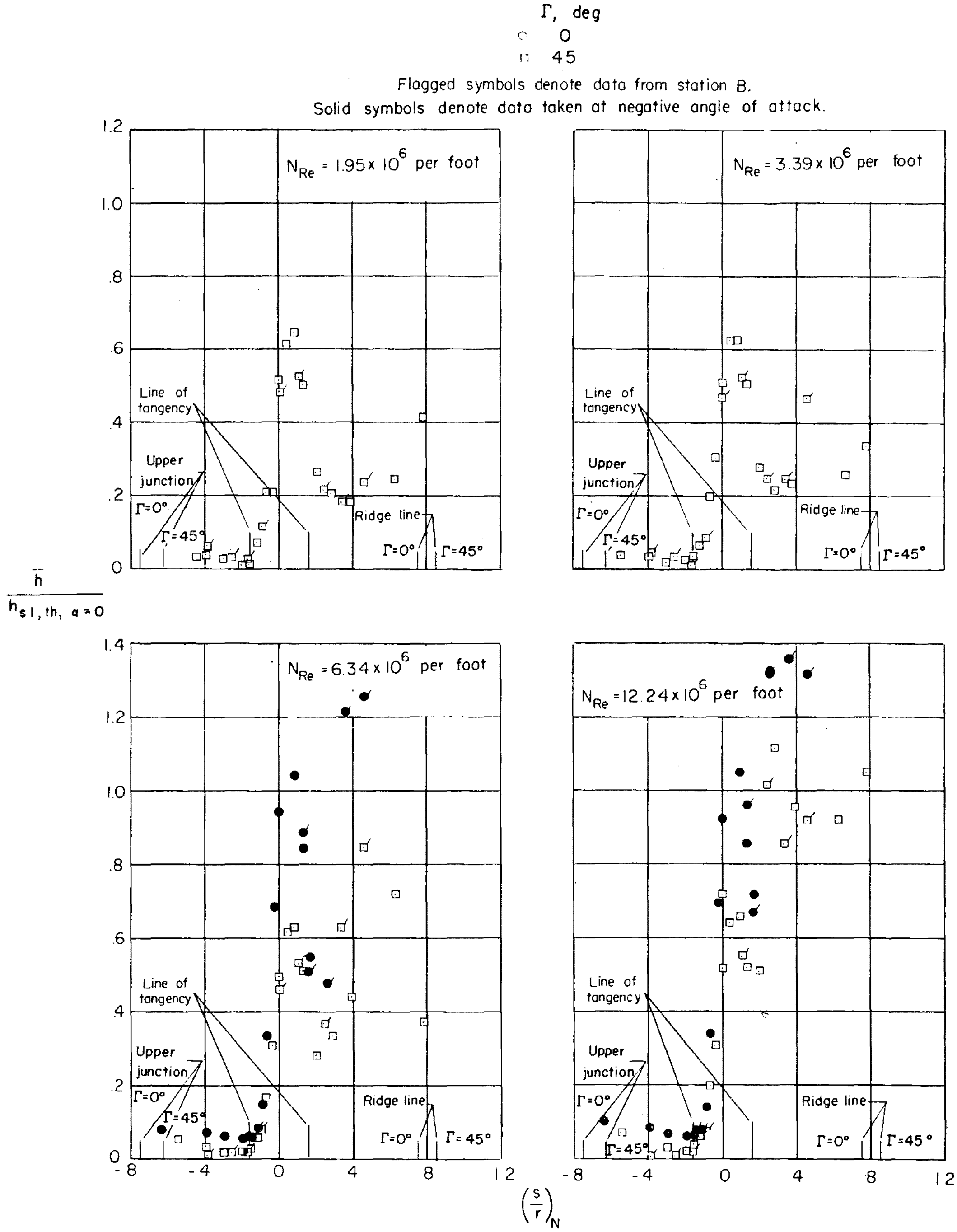

(d) $\alpha = 15^{\circ}$.

Figure 7.- Continued.

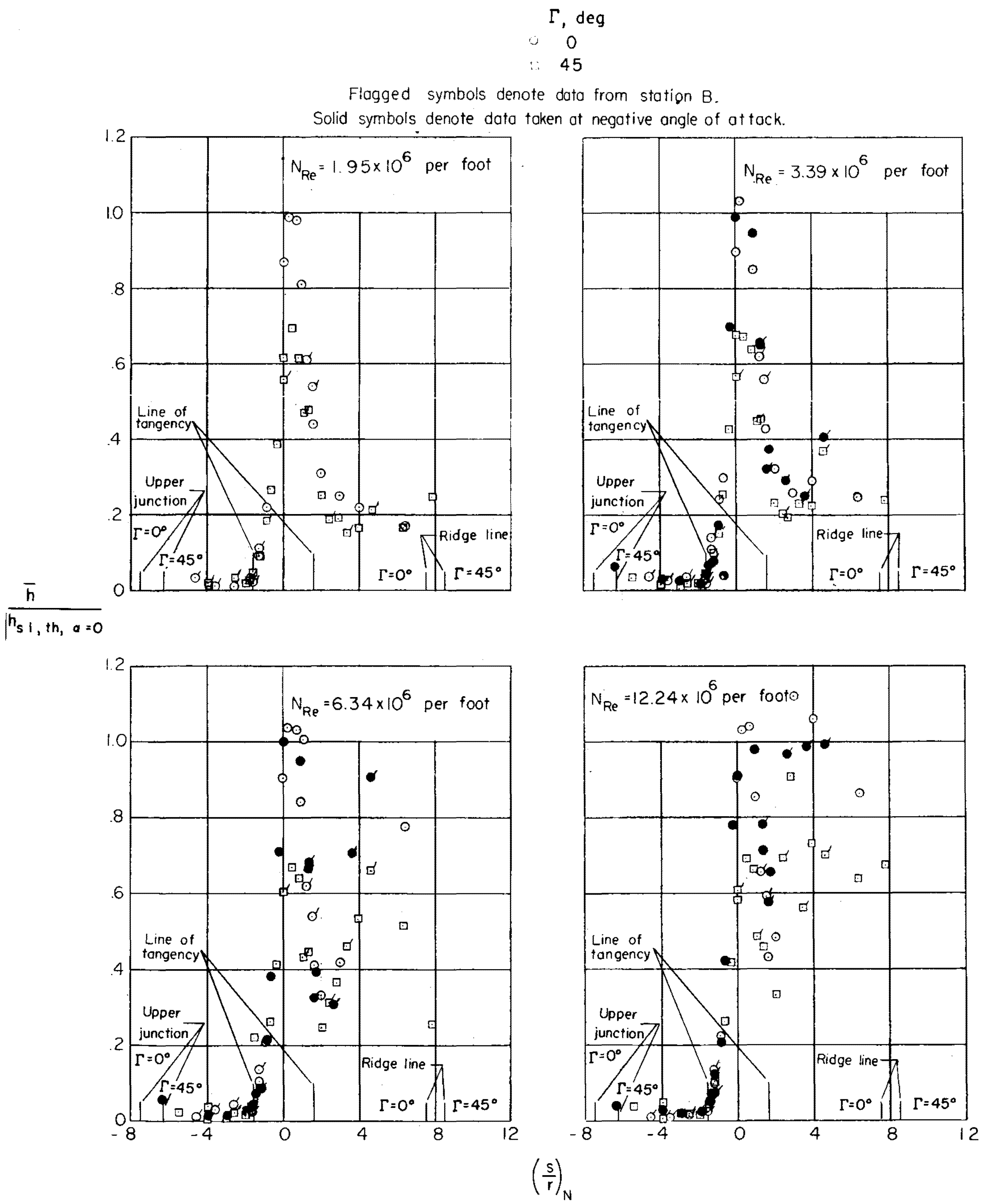

(e) $\alpha = 20^{\circ}$.

Figure 7.- Concluded.

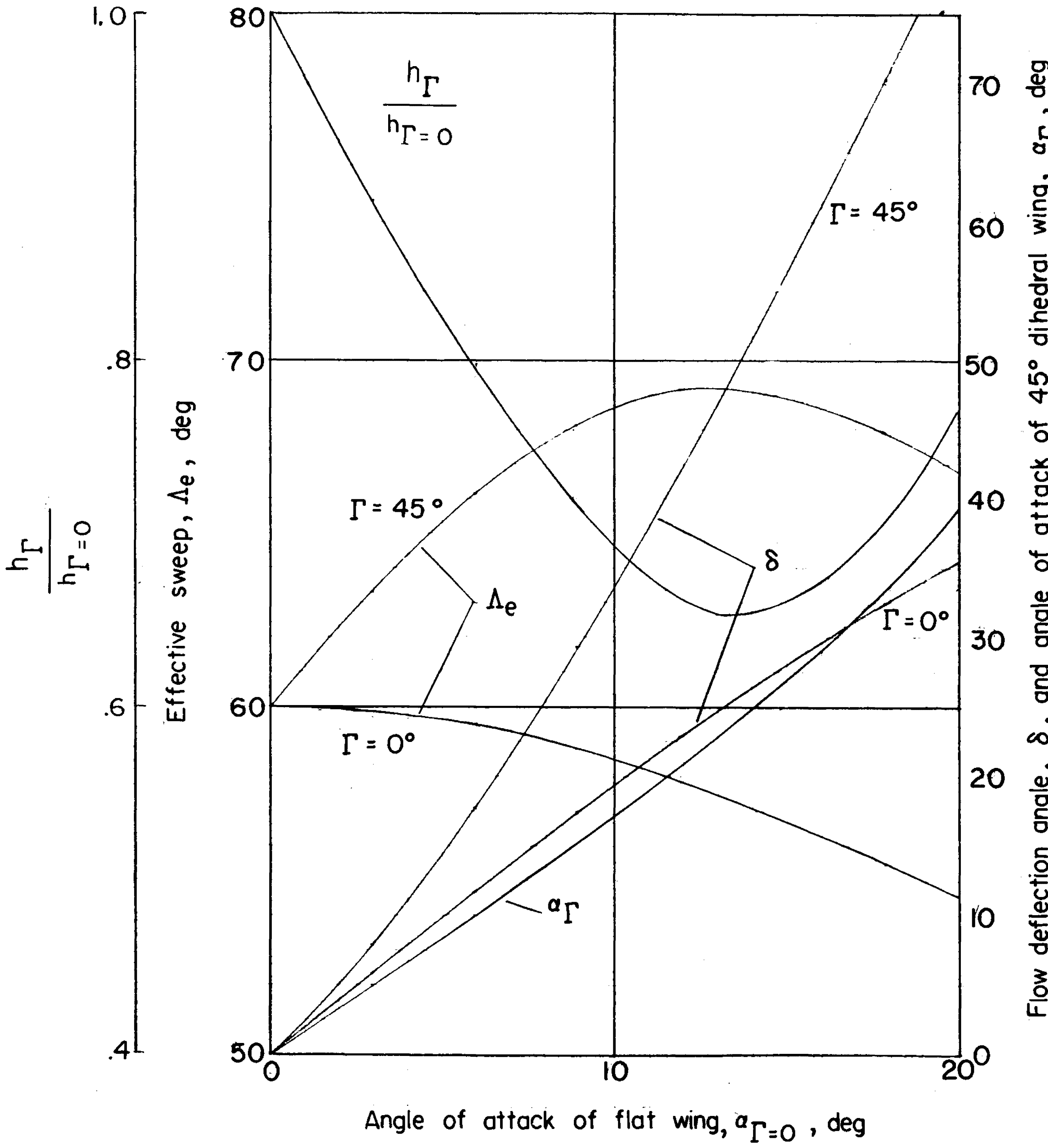

Figure 8.- Variation of wing effective geometry with angle of attack of flat wing for equal lift of the flat wing and 45° dihedral wing.

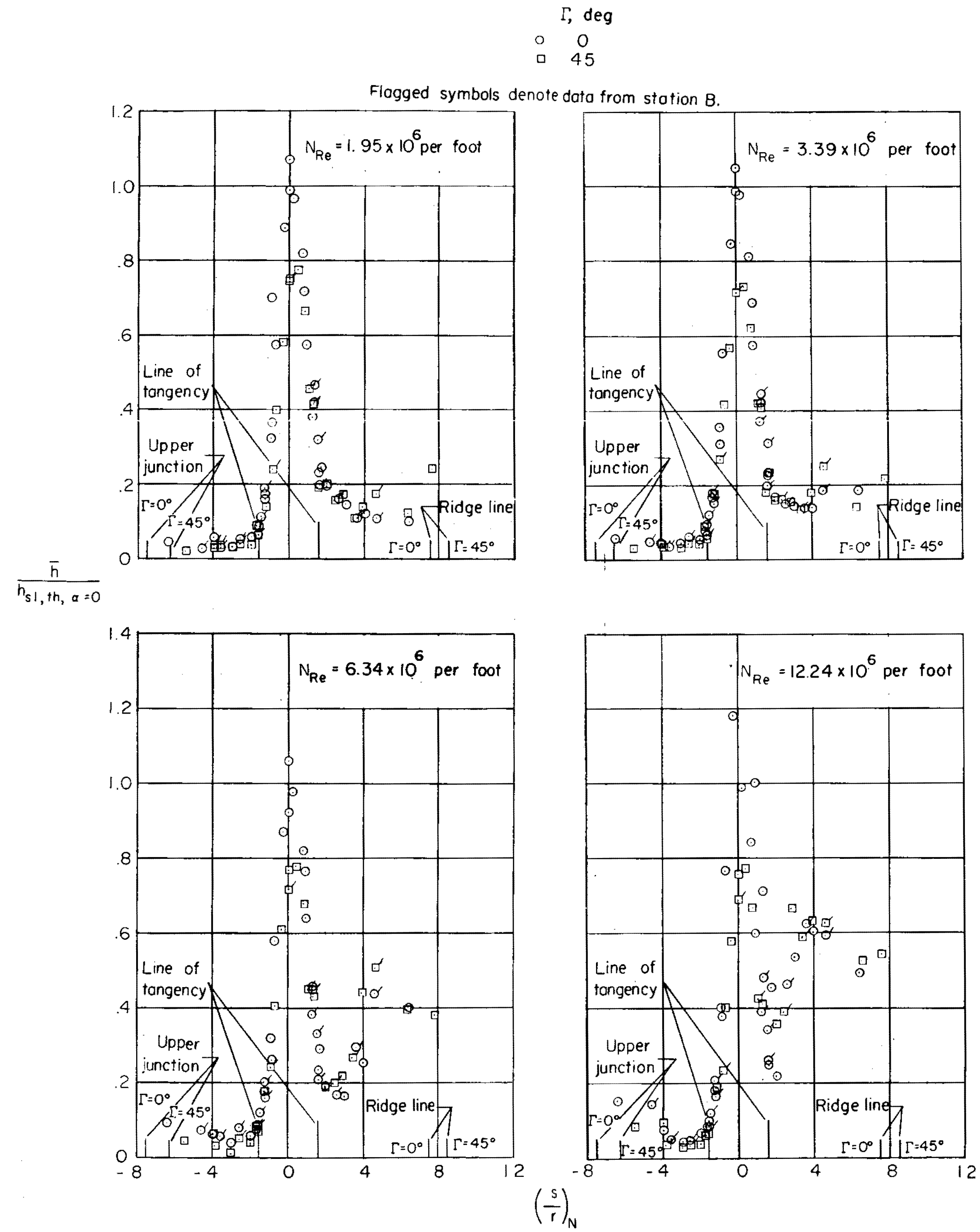

(a) $C_L = 0.021$.

Figure 9.- A comparison of the heating rates to the 0° and 45° dihedral wings at equal lift and equal unit Reynolds numbers.

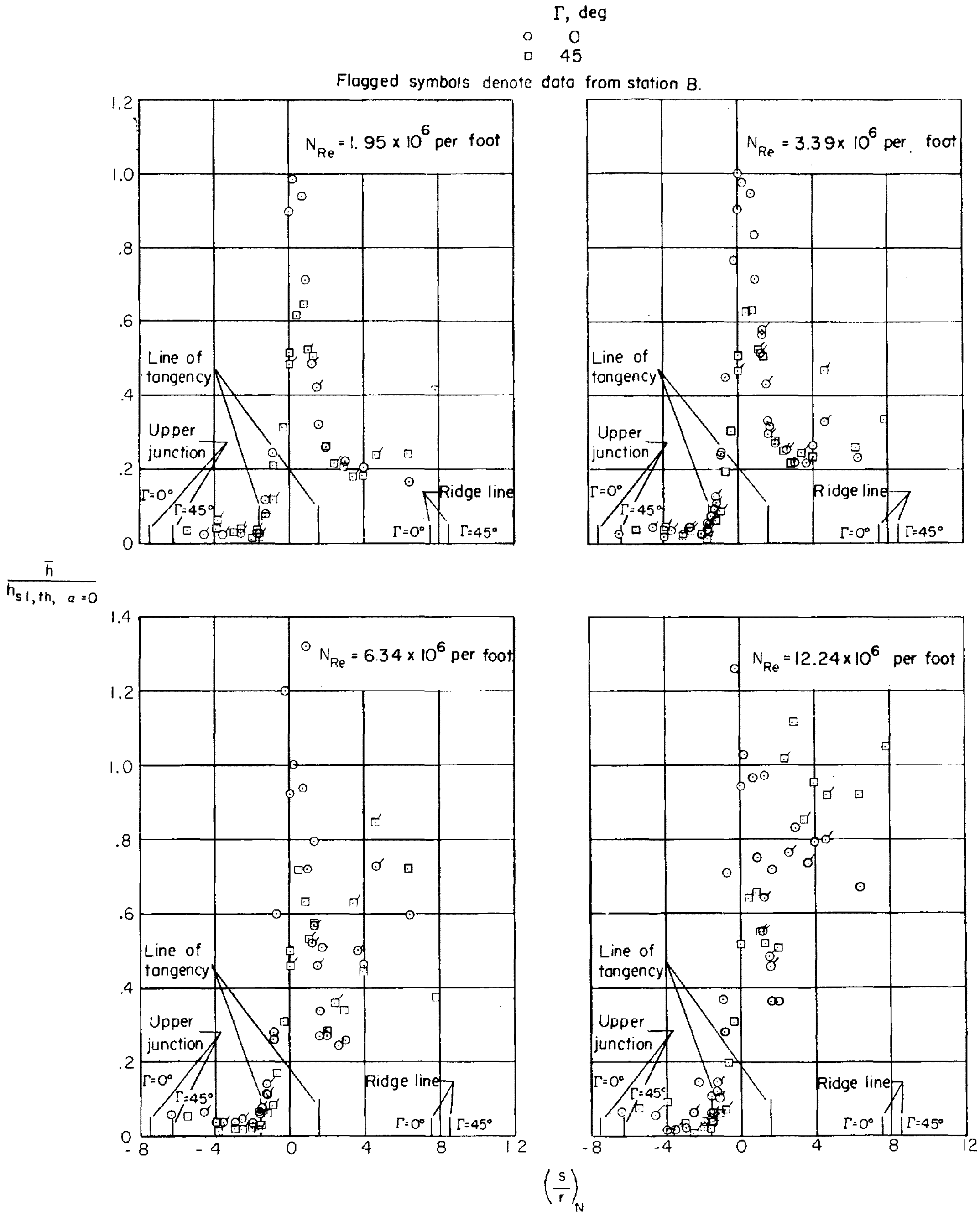

(b) $C_L = 0.078$.

Figure 9.- Concluded.